

Auxetic oesophageal stents: structure and mechanical properties

Murtaza Najabat Ali · James J. C. Busfield ·
Ihtesham U. Rehman

Received: 26 February 2013 / Accepted: 9 October 2013 / Published online: 20 October 2013
© Springer Science+Business Media New York 2013

Abstract Oesophageal cancer is the ninth leading cause of malignant cancer death and its prognosis remains poor, ranking as the sixth most frequent cause of death in the world. This research work aims to adopt an Auxetic (rotating-squares) geometry device, that had previously been examined theoretically and analysed by Grima and Evans (J Mater Sci Lett 19(17):1563–1565, 2000), to produce a novel Auxetic oesophageal stent and stent-grafts relevant to the palliative treatment of oesophageal cancer and also for the prevention of dysphagia. This paper discusses the manufacture of a small diameter Auxetic oesophageal stent and stent-graft. The oral deployment of such an Auxetic stent would be simplest if a commercial balloon dilatational catheter was used as this obviates the need for an expensive dedicated delivery system. A novel manufacturing route was employed in this research to develop both Auxetic films and Auxetic oesophageal stents, which ranged from conventional subtractive techniques to a new additive manufacturing method. Polyurethane was selected as a material for the fabrication of Auxetic films and Auxetic oesophageal stents because of its good biocompatibility and non-toxicological properties. The Auxetic films were later used for the fabrication of seamed Auxetic oesophageal stents. The flexible polyurethane tubular grafts were also attached to the inner luminal side of the seamless Auxetic oesophageal stents, in order to

prevent tumour in-growth. Scanning electron microscopy was used to conduct surface morphology study by using different Auxetic specimens developed from different conventional and new additive manufacturing techniques. Tensile testing of the Auxetic films was performed to characterise their mechanical properties. The stent expansion tests of the Auxetic stents were done to analyse the longitudinal extension and radial expansion of the Auxetic stent at a range of radial pressures applied by the balloon catheter, and to also identify the pressure values where the Auxetic stent fails. Finite element models of both Auxetic film and Auxetic stent were developed, and the results were compared with experimental results with a good agreement. The tensile testing of the Auxetic polyurethane films revealed that the Poisson's ratio of the sample ranged between -0.87 and -0.963 at different uniaxial tensile load values. From the stent expansion test, it was found that the Auxetic oesophageal stent radially expanded from 0.5 to 5.73 mm and longitudinally extended from 0.15 to 1.83 mm at a range of applied pressure increments (0.5–2.7 bar) from the balloon catheter.

1 Introduction

Squamous cell carcinoma can occur anywhere along the length of the oesophagus because squamous cells cover the entire oesophagus [1]. Both benign and malignant epithelial tumours take place in the oesophagus, and most of the benign tumours are not epithelial in origin and occur from other layers of the oesophageal wall. Dysphagia and its concomitant weight loss are generally considered to be signs of a more advanced stage, by which at least 50 % of the oesophageal lumen is compromised and is causing

M. N. Ali (✉) · I. U. Rehman
Department of Materials Science and Engineering, The Kroto
Research Institute, The University of Sheffield, North Campus,
Broad Lane, Sheffield S3 7HQ, UK
e-mail: murtaza_bme@hotmail.com

J. J. C. Busfield
Department of Materials, Queen Mary University of London,
Mile End Road, London E1 4NS, UK

obstruction to the free passage of the alimentary bolus. As a result, dysphagia is seen as a sign of a poor prognosis [2].

The oesophagus is an expandable muscular tube which is protected by the upper and lower oesophageal sphincter at both ends [3]. The information from the histological studies suggests that oesophageal wall can be analysed from a mechanical point of view, as a multilayered anisotropic composite. Due to the specific orientation of reinforcing fibres each layer of the oesophageal wall is characterized by anisotropic behaviour. Oesophageal tissue has mechanical properties which are non-linear and anisotropic [4, 5]. Peristaltic propulsive forces in the oesophagus were measured by [6, 7], using a force transducer. Both symptom free (healthy) and dysphagia groups were investigated for oesophageal force measurements. In the first study between healthy and dysphagia group, the oesophageal force values obtained were the largest [50 g (force)] in the lower third of the oesophagus. In the middle one-third of the oesophagus the force values declined [approx. 30 g (force)], and lowest force values were recorded in the upper one-third [approx. 20 g (force)] [6]. The second study was performed in only healthy patients by [7], and it was clear from the results that peristaltic force of the oesophagus increased directly with sphere size of the transducer and was greatest at the most distal oesophageal level [approx. 125 g (force)]. It is believed that increase in muscle mass may fairly explain the distal increase in oesophageal peristaltic activity [7]. Oesophageal stents have been in use as a palliative method for the patients suffering from advanced stage oesophageal cancer and also for the relief of dysphagia [8]. There are still problems in currently available self-expanding metals and plastic stents, which are associated with high rates of early and late complications. The major early complications reported in oesophageal stents are migration, perforation, and haemorrhage and are noticed in up to 6, 7 and 6 % patients respectively. Whereas long term oesophageal stenting is associated with high rates of bleeding, tumour overgrowth, migration, fistula formation and bolus impaction, and these rates are reported as 19, 36, 33, 5 and 23 % respectively [9].

Auxetic structures as discussed by [10], have a counter-intuitive behaviour and exhibit the very unusual property of becoming wider transversely when stretched longitudinally, that is they possess negative Poisson's ratio. The Poisson's ratio is defined as the negative ratio of the transverse strain and the axial strain in the direction of loading. All common materials have positive Poisson's ratio, which implies that the materials contract transversely under uniaxial extension, or expand laterally when in compression. The direction of expansion and contraction being reversed in Auxetic structures.

A new mechanism was theoretically proposed by [10] to achieve a negative Poisson's ratio which was based on an

arrangement involving rigid squares connected together at their vertices by hinges. As each unit cell contains four squares, each square contains four vertices, and two vertices correspond to one hinge. It was previously derived in the analytical models reported by [11, 12], where the mechanical behaviour of the Auxetic (rotating-square) geometry was theoretically presented.

The main focus of this research work was to adopt a novel manufacturing approach comprising of both conventional subtractive and new additive manufacturing techniques, for the production of both seamless and seamed Auxetic stents and stent-grafts. This study also endeavoured to manufacture a significantly small diameter Auxetic oesophageal stent and stent-graft. In order to easily deploy the Auxetic stent orally using a commercial balloon dilatational catheter, and hence it also obviates the need of an expensive dedicated delivery system. This new oesophageal stent technology is also believed to reduce both early and late complications associated with self-expanding metallic stents. The major early complications of the commercially available stents are migration, perforation and haemorrhage, which can be minimised by the synclastic (the tendency to bulge out) plastic deformation of the stent, good mesh and soft polymeric edges respectively. Similarly, the major long term complications of commercially available self-expanding stents are tumour overgrowth, bleeding and fistula formation. Where tumour overgrowth can be reduced by radial and longitudinal expansion of the Auxetic stent, bleeding and fistula formation can be avoided by soft polymeric edges and an internal luminal graft can be useful to stop tumour ingrowth and to cover any fistula. There has been no study reported in the literature so far concerning to the fabrication of Auxetic stents or a stent-graft based on rotating-squares geometry and their physical micro-structural/mechanical analysis or finite element analysis. There is only one earlier reported study [13], where the fabrication of a seamed Auxetic stent was attempted using a laser cutting technique and the tensile testing of Auxetic films was conducted.

Therefore, the purpose of the present study is to analyse the surface morphology of the Auxetic oesophageal stents developed from a range of manufacturing techniques, and to mechanically characterise the Auxetic stents and films (which were used in the seamed fabrication of the stents) in a fashion which is more relevant to Auxetic stent expansion and behaviour within oesophagus. Finite element analysis of both the Auxetic film model and Auxetic stent model was performed to correlate and validate the physical tests with FEA modelling results. Since the oesophagus is a large conduit subjected to large radial forces, it was anticipated that a more bulky scaffold such as an Auxetic (rotating-squares) stent-graft would be effective for maintaining the lumen of the cancerous oesophagus patent.

2 Materials and methodology

To develop a polymeric Auxetic (rotating-squares) geometry and to configure it into a film and tubular stent form, polyurethane was selected. Polyurethane due to its biocompatibility and non-toxicological behaviour has been widely adopted in biomedical applications. Polyurethane is a very attractive choice, as their physicochemical properties can be tailored by changing the ratio of soft segment to hard segment and their respective chemistries to suit the intended application. Allowing several different commercial rigid plastic polyurethane materials to be adopted to construct the Auxetic (rotating-squares) geometry into a film and also into a tubular stent-graft configuration. The Auxetic (rotating-squares) geometry selected followed the theoretical predictions of [10] and emulates the natural cellular framework of zeolites. Recent studies [11] have helped derive the analytical model describing the mechanical behaviour and to demonstrate that the mechanical properties depend on the relative magnitude of the stretching and hinging constants, the square dimensions and the angle between the squares, and by changing the



Fig. 1 Lasercut Auxetic polyurethane film

Fig. 2 Titanium reverse-Auxetic mould made by (CAD to metal based) EBM process



magnitude of applied force and geometry, the value of Poisson's ratio can be controlled.

2.1 Lasercutting of polyurethane

The same thermo-mechanical cutting method by computerised numerical control (CNC) guided laser was adopted which was reported earlier for the fabrication of Auxetic polypropylene films [13]. The lasercutting of polyurethane films was carried out on a reasonably small scale. Thermo-plastic polyurethane commercially known as "Pellethane" was supplied by Smith & Nephew UK Ltd., which was an aromatic polyether, based polyurethane material and these rigid polyurethane films were manufactured specifically for medical applications. The polyurethane films were 500 μ thick and the hardness of the films was 75 Shore 'D'. For the fabrication of an Auxetic (rotating-squares) polyurethane film as shown in Fig. 1, an Epilog laser LEGEND Mini-18 CNC guided system was used. The laser system used laser power of around 30 W to cut the workpiece material.

2.2 Polyurethane casting

Auxetic polyurethane films were also made by casting polyurethane onto a metal reverse-Auxetic mould fabricated by an Electron Beam Melting (EBM) technique. The EBM process is an additive manufacturing technique capable of producing fully dense titanium alloy products with extremely complex geometries. Initially, a 3D CAD design was created by using Autodesk INVENTOR software, which involved an inverted-Auxetic die plate having the recessed rotating-squares and protruding diamond-shaped units. The ARCAM EBM S12 (CAD to metal) based system as shown in Fig. 2 was used, which physically reproduced the computer slices by melting metal powder layer by layer. Titanium (Ti6Al4V) metal powder was used which had spherical particles ranging from 45 to 100 μ in diameter. The ARCAM EBM technology depends on the use of a high power electron beam to provide the

required energy to melt powdered titanium alloy in an additive fashion. An electron beam having 4.8 kV and 17 mA was used to melt the titanium powder into solid metal. This process was executed in a vacuum of approximately 1×10^{-3} mbar in the build chamber and around 1×10^{-6} mbar in the electron beam gun where the electron beam was generated. A 60 kV accelerating voltage was supplied to the anode located underneath the electrode, which accelerated the emitted electrons in the desired direction.

The electron beam was focused using an electromagnetic coil, and subsequently electromagnetic steering coils were used to deflect the focused electron beam to the desired spot on the powder bed. As there were no moving parts within the system, the electromagnetic steering coils were able to sweep the focused electron beam at 500 mm/s speed. The EBM process was initiated by the distribution of a 100μ thick layer of fine Ti6AL4V powder on a steel platform. Subsequently, an electron beam scanned the areas in x and y axes within the build chamber on the powder bed as defined by the CAD model, and then completely melted the powder in the scanned areas. After which the steel platform was lowered by 100μ along z-axis, and a new layer of powder was distributed on top of the previously melted layers. The EBM process was running continuously layer by layer until a complete part was produced. The completed titanium part was then inserted into ARCAM Powder Recovery System to remove any excess powder that surrounded the part produced in the ARCAM EBM process. The powder recovery method involved minimal dust generation for safe operation, and a closed loop material recovery and elimination of fine particles as shown in Fig. 3. The surface of the recovered

titanium mould appeared to be rough and grained after cleaning of the mould from the metal powder covering. Therefore, surface roughness of the titanium mould was reduced using a conventional mechanical finish machining method. The titanium mould prepared by CAD to Metal based EBM process, was then finally ready for film casting.

Auxetic polyurethane films were prepared subsequently by a casting method which involved, taking the two parts of the SmoothCast-60D polyurethane resin in a volumetric ratio of 1:1, degassing first the two parts separately for 15 min in a vacuum chamber at 760 mmHg pressure, mixing the two parts in one container and then degassing again the polyurethane mixture for 3 min, preparing the titanium mould for casting by coating it with CilRelease

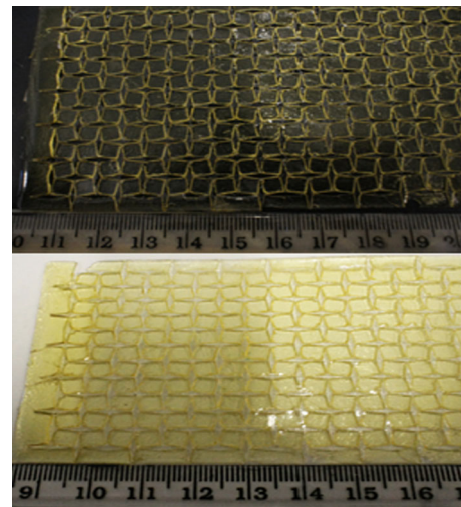


Fig. 4 Auxetic polyurethane film prepared from metal reverse-Auxetic mould

Fig. 3 Recovery of the metal powder that surrounded the part (reverse-Auxetic mould) produced from EBM process

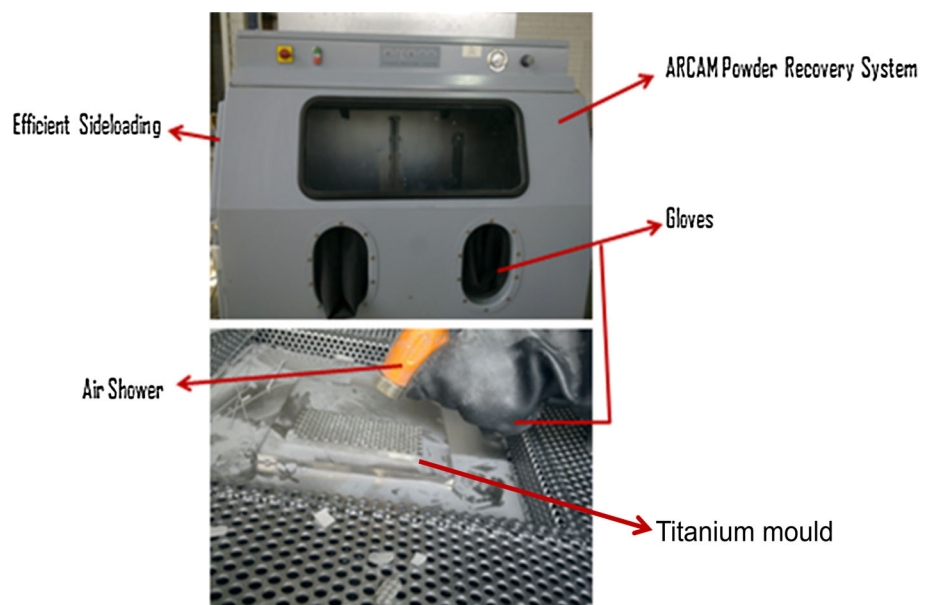


Fig. 5 **a** Two halves of the titanium collapsible tubular and **b** the components of the collapsible tubular die



1812E silicone based mould release agent and finally dispensing the polyurethane onto the titanium reverse-Auxetic mould for casting. Scraping was carried out to remove excess material from the surfaces of the diamond-shaped parts in the mould, and then the cast polyurethane was left to cure. After 2 h the polyurethane Auxetic film was peeled off carefully from the titanium mould (Fig. 4).

2.3 Development of Auxetic stent

2.3.1 Collapsible mould

For the development of an Auxetic polyurethane (semi-rigid) stent, a collapsible tubular die was fabricated using the EBM process. The collapsible tubular die was designed in two halves having the same reverse-Auxetic pattern of protruding diamond-shaped bits and recessed rotating-square parts at the luminal side of the collapsible tubular die. The EBM process used titanium (Ti6Al4V) alloy powder for the fabrication of the two halves of the collapsible tubular die (in Fig. 5a). The main reason for using a titanium collapsible tubular die was, to avoid the adhesion of the cast polyurethane onto the tubular die material. The components of the collapsible tubular die such as rings, funnel, internal rod, and a support were then built using stainless steel (Fig. 5b).

The same two part semi-rigid SmoothCast-60D polyurethane resin was used to cast into the metal collapsible tubular die. The casting process involved, degassing of the polyurethane material, coating of the collapsible tubular die with CilRelease 1812E silicone based mould release agent, and finally dispensing the polyurethane into the funnel located at the top of the tubular die following by the continuous stirring to push the material into the tubular die



Fig. 6 A fractured Auxetic polyurethane stent having being released from the tubular die

cavity. When the collapsible tubular die was completely filled with the polyurethane material throughout its length, it was left to cure for 2 h. Post curing, it was found very difficult to open the tubular die and to remove the Auxetic stent, mainly because of the reason that the cast polyurethane was very stiff and did not provide any flexibility to break the vacuum and to allow the two halves of the tubular die to open. Consequently, the Auxetic polyurethane stent when removed from the titanium collapsible tubular die was ruptured in a number of locations, and the fabrication of a seamless Auxetic polyurethane stent by this method was not successful as shown in Fig. 6.

2.3.2 Vacuum casting

Vacuum casting recently adopted to manufacture functional plastic prototypes within a few hours was also

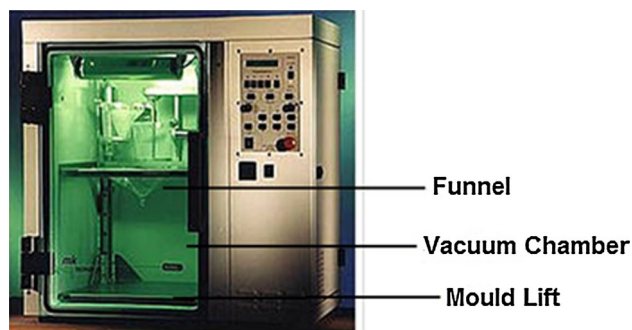


Fig. 7 MK technology basic model SYSTEM-1 with mould lift and vacuum chamber

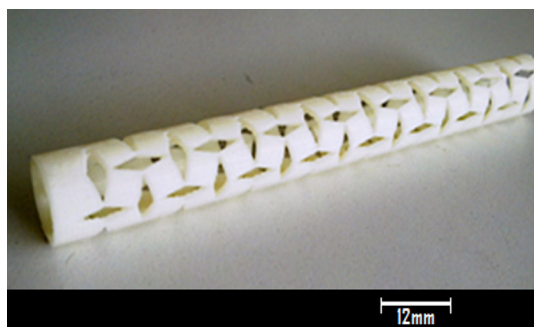


Fig. 8 Master model of the Auxetic stent made by FDM process

investigated to develop a seamless Auxetic stent. The MK Technology basic model SYSTEM-1 was used, which is design for prototype production. This system comes with a mould lift which helps to adapt the position of the mould exactly to the funnel as shown in Fig. 7.

A pre-requisite for vacuum casting with the desired polymer material, is a perfect master model which can be made conventionally or by one of the new generative techniques like stereo-lithography, fused deposition modelling (FDM) or layer laminate manufacturing. While developing a master model every detail of the actual part should be considered, so that the master model can be duplicated with a desired material by the help of vacuum casting process. The surface of the master model must be free from defects. The 3D design of the Master model (Auxetic stent) had 13 mm outer diameter and 120 mm length which was exported to the FDM INSIGHT software for part production. The part was produced by FDM rapid-prototyping process using acrylonitrile–butadiene–styrene material (Fig. 8).

In the first step, the mould making process was prepared by determining the required contours and separation lines. For the preparation of the mould, a casting frame was required which was made quickly and inexpensively from Melamine coated chip boards glued together using glue. In the second step, the gates and risers were adjusted and the

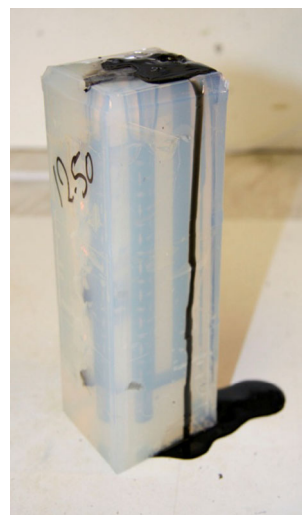


Fig. 9 Polyurethane casted into a silicone mould

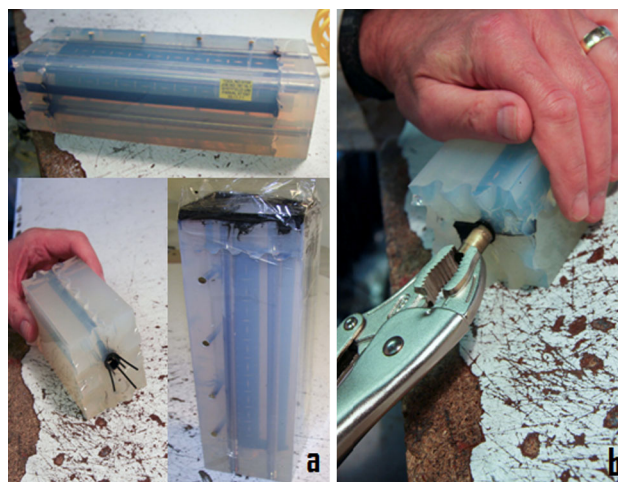
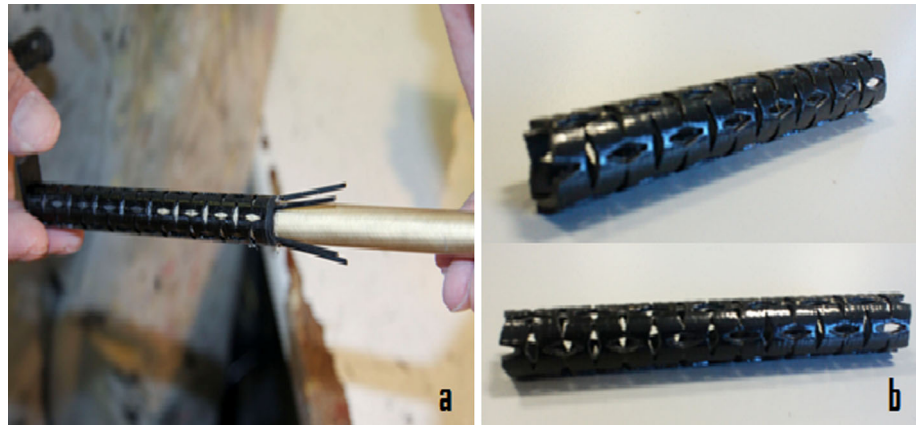


Fig. 10 **a** Auxetic polyurethane stent suspended with gates and risers inside the silicone mould, and **b** the Auxetic stent and metal rod are being extracted

casting frame was ensured to be big enough to allow an all-around covering of the Master model with a silicone layer of at least 2 cm. Subsequently, the prepared Master model with gates and risers was suspended inside the casting frame, and the solid metal rod of the same dimensions was inserted inside the Master model. The necessary amount of silicone which had been calculated from the mould volume was weighed in a plastic container and 10 % hardener was added. When the silicone and hardener were mixed together for 2 min, the mixing time was recorded, as this was the time when the Pot Life of 90 min began. For the preparation of mould, the silicone must be completely degassed because the remaining gas particles with in the mould expand under vacuum which effects the dimensional stability of the cast.

Fig. 11 **(a)** Metal rod is being separated from the Auxetic stent, and **(b)** rigid Auxetic Polyurethane stent [14]



The silicone was carefully poured into the casting frame from one side after degassing. The casting frame was completely filled and the Master model was covered by a layer of silicone. When silicone was hardened, the casting frame was removed from the oven, and the compressed air was blown inside the mould through the gate to remove the Master model evenly from the mould leaving the metal rod inside the casting cavity of the silicone mould. Subsequently, the mould was then ready for casting polyurethane material. The rigid PX 212 two part polyurethane resin (acquired from Axson UK Ltd.) of 76 shore D hardness was used for part production. Initially, the polyurethane casting resin was pre-degassed for about half an hour. The mould was then placed inside the vacuum chamber on the mould lift, and the polyurethane pre-degassed mixture was poured into the mould through funnel. The chamber was completely evacuated and the mould was taken out of the chamber, and for the quick hardening of the resin the mould was heated at 65–70 °C for 2 h. The cast polyurethane within the mould was then taken out of the oven and left for further curing at room temperature for 15 min as shown in Fig. 9.

Once the casted polyurethane was completely hardened inside the mould, scalpel and pressurised air were used for effective parting of the mould. The mould was then slightly opened from the side, and the casted polyurethane tube with a metal rod was taken out manually using pliers as illustrated in Fig. 10b.

The Auxetic stent was finally separated from the metal rod by simply sliding the rod out as shown in Fig. 11.

The same vacuum casting process was repeated using Master models of different dimensions, i.e. the outer diameter was 10 mm, the length was 120 mm, and the wall thickness was 0.5 mm. Different VC-3300 three part polyurethane resin of 95 shore A hardness was also used to cast into this silicone mould. Consequently, a semi-flexible Auxetic stent was fabricated which exactly replicated the Master model without any defects (Fig. 12).

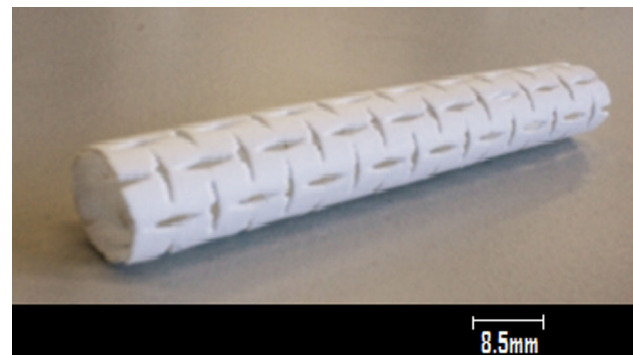


Fig. 12 Semi-flexible Auxetic polyurethane stent

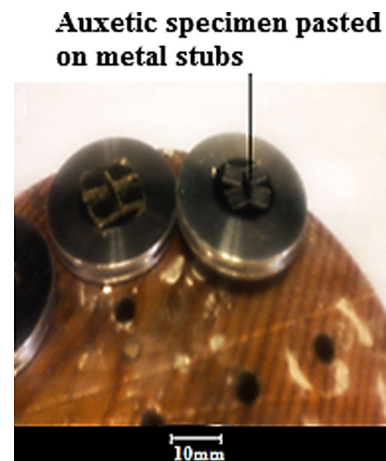


Fig. 13 Auxetic unit-cells fixed on metal stubs for subsequent sputter coating process and SEM

2.4 Topographical characterisation

The topographical characterisation of the Auxetic (rotating-squares) geometry fabricated by different manufacturing techniques was carried out by using scanning electron

microscopy (SEM). Single unit-cells (comprising of four rotating-squares) were obtained from both the Auxetic films and the Auxetic stents, and were used for SEM. Initially, Auxetic unit cells were taken from each fabrication method, and then the single unit-cells were fixed on a circular metal stub for subsequent sputter coating as shown in Fig. 13 to create suitable surface conductive properties. To achieve this, all specimens were gold coated by using Emscope SC500 sputter coater in 0.05 Torr vacuum. The coating process of each sample spanned around 3 min at 15 mA. Finally, the SEM images were taken at 40 and 80 times magnification using a secondary electron at 1,500 kV, and these were used to monitor and evaluate production quality of the Auxetic (rotating-squares) geometry from the various different fabrication techniques.

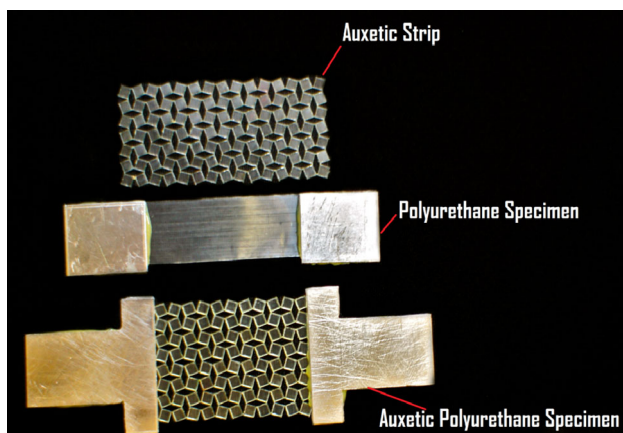


Fig. 14 Polyurethane and Auxetic polyurethane specimens prepared for testing

2.5 Mechanical characterisation

2.5.1 Tensile test

Tensile testing of the developed Auxetic polyurethane films based on the rotating-squares geometry was performed to characterise their mechanical properties and to determine their elastoplastic behaviour, and the mechanical data collected from this test was further used in the finite element analysis.

The tensile testing was carried out using the Auxetic polyurethane films developed by lasercutting process. Initially an A4 size polyurethane film was used to prepare the polyurethane strips according to the ISO 527-3 standard, in order to measure the baseline tensile data of the polyurethane material. Therefore, three non-Auxetic polyurethane specimens were prepared by carefully cutting the A4 size polyurethane film 100 mm long and 20 mm wide. The steel strips of 25 mm length and 20 mm width were prepared for the adhesive by abrading the surface of the steel strips to achieve good adhesion with polyurethane specimens. The adhesive was applied on the steel strips, and the two sides of the polyurethane specimen were then enclosed within the two steel strips placed parallel to each other on either sides of the polyurethane specimen. The polyurethane specimen having metal strips on both sides were prepared to ensure a good grip in the tensile testing machine (in Fig. 14). Therefore, the gauge length, thickness, and width of the polyurethane specimens were 50, 0.5, and 20 mm respectively. Similarly, three Auxetic polyurethane specimens were prepared by carefully cutting the Auxetic film 80 mm long and 31.5 mm wide. The T-shaped steel plates were made and subsequently attached to the both sides of the Auxetic polyurethane specimen to improve the grip between testing machine and specimen. Therefore, the gauge length,

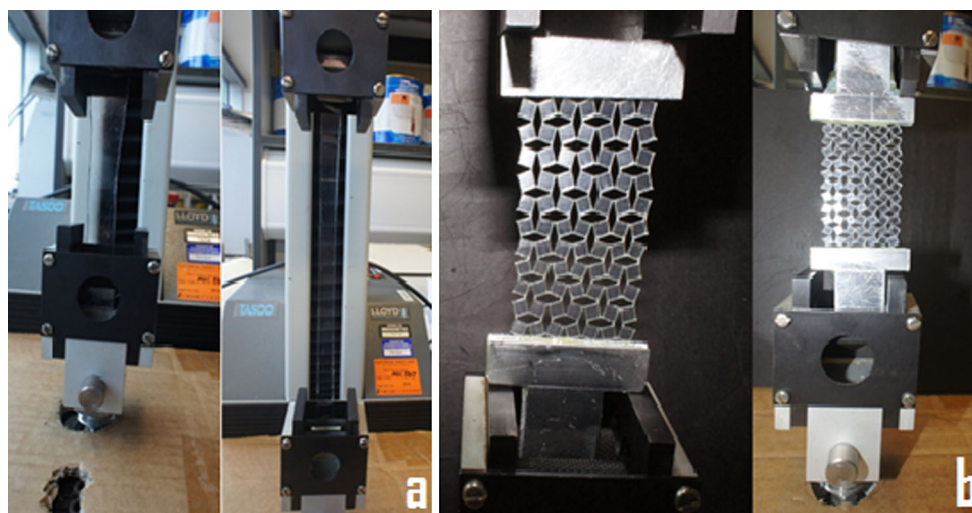


Fig. 15 **a** Polyurethane specimen subjected to tensile loading, and **b** uniaxial tensile load is applied to the Auxetic polyurethane specimen

thickness, and width of the Auxetic polyurethane specimens were 50, 0.5, and 31.5 mm respectively.

A Lloyds Instruments TA500 tensile tester with 500 N load cell was used for this study. The equipment was initially calibrated and the polyurethane specimen was mounted tightly between the threaded grips of the tester. The polyurethane specimen was subjected to uniaxial tensile load at 5 mm/min crosshead speed until the point of failure as shown in Fig. 15a. The same test was repeated twice and the mean of the baseline stress–strain data was taken and the acquired true stress and plastic strain values were used as the prescribed elastic–plastic material data for the FEA model. After getting the baseline data, the Auxetic polyurethane specimen was tested in uniaxial tension at 5 mm/min cross head speed until the point of failure shown in Fig. 15b. This test was carried out by applying uniaxial tensile load manually to the Auxetic polyurethane specimen in such a fashion that the longitudinal and transverse extensions of the specimen were measured at every load increment until the point of failure. The longitudinal and transverse extension values of the Auxetic specimens obtained at different loads were used to determine their elastic–plastic deformation behaviour and their Poisson’s ratio (ν). Another Auxetic polyurethane sample was then subsequently subjected to uniaxial tensile loads at 5 mm/min cross head speed until the point of failure, and the longitudinal extension of the specimen was measured and

stress–strain graph was acquired directly from the tensile tester at different load values.

2.5.2 Stent Expansion Test

It was envisaged, that the deployment of the Auxetic oesophageal stent-graft will be without a dedicated delivery system. This will be administered orally into the oesophagus using a small diameter Auxetic stent-graft with a balloon dilatational catheter as illustrated in Fig. 16. The balloon dilatational catheter has already been in use for the pre-dilation of the oesophageal lumen and for the post-dilation of the commercial oesophageal stents.

Therefore, an expansion test was conducted which involved the expansion of the Auxetic stents and stent-grafts using different sized commercial balloon dilatational catheters. The semi-rigid and rigid Auxetic stents and stent-grafts



Fig. 16 A schematic showing an Auxetic stent mounted on a balloon catheter

Fig. 17 **a** Semi-flexible Auxetic stent and stent-graft, and **b** rigid Auxetic stent and stent-graft

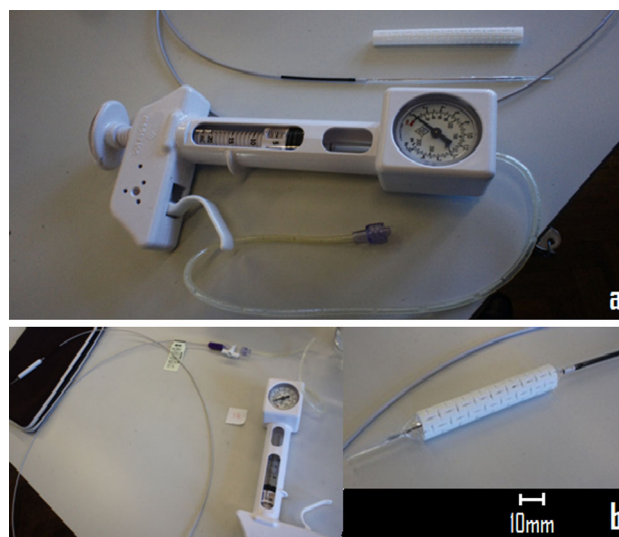
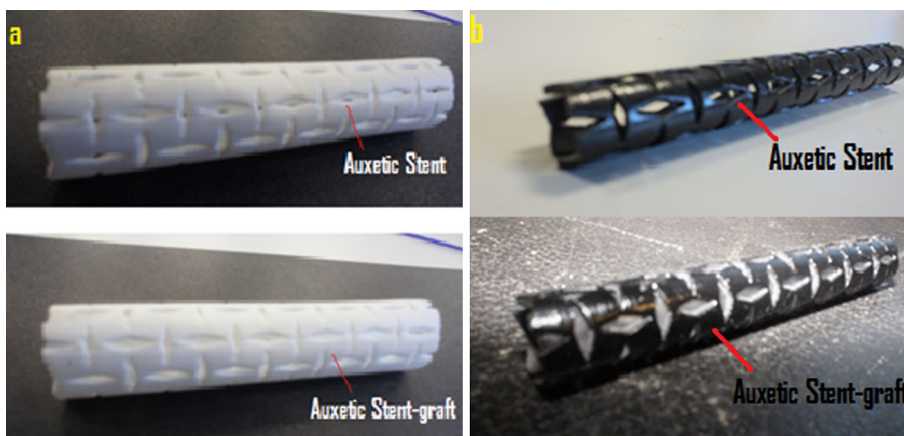


Fig. 18 **a** Auxetic stent with inflation device and catheter, and **b** the balloon holding the stent tightly in place by applying a small initial radial pressure

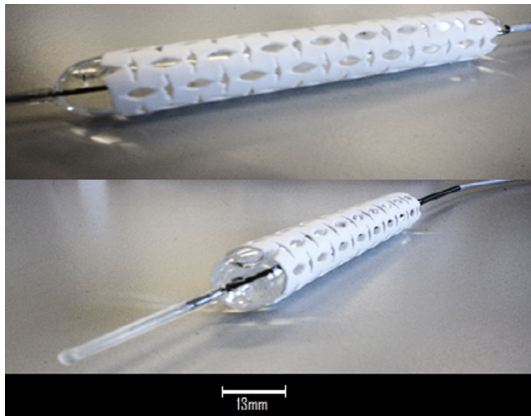


Fig. 19 Semi-flexible Auxetic stent being expanded by balloon

made of polyurethane material using vacuum casting process, were employed in these expansion test as shown in Fig. 17.

In Test-I, a semi-rigid Auxetic stent; 50 mm length, 10 mm outer diameter and 0.5 mm wall thickness, was investigated using MEDFLATOR-II inflation device (Smiths Medical Deutschland GmbH) and CRE wireguided balloon dilatational catheter (18, 19 and 20 mm diametrical range) of 55 mm balloon length (supplied by Boston Scientific UK). Initially, the Auxetic stent was mounted on the balloon catheter in such a way that the stent was placed in the middle of the balloon. The inflation device with a built-in manometer was filled with water and was subsequently connected to the balloon catheter. A slight pressure of 0.2 bar was initially applied, so that the balloon would hold the stent tightly in place (in Fig. 18b). The test was then initiated by the application of small pressure increments from the inflation device. Subsequently, the radial pressures were increased in steps with both the axial length and the diameter of the stent being recorded at every pressure increment, until the point of stent failure.

In Test-II, the procedure was the same as Test-I; however, the specifications were modified as the semi-flexible Auxetic stent was mounted on different sized balloon catheters (10, 11 and 12 mm diametrical range) each having a balloon length of 80 mm (supplied by Boston Scientific UK). The Auxetic stent was 68 mm in length and the outer diameter was 10 mm (in Fig. 19). The radial pressures were applied in the same way and the changes in length and diameter of the stent were recorded at each pressure increment.

The Test-III involved the same prior procedure, but the specifications were changed as the rigid Auxetic stent was mounted on a balloon catheter (18, 19 and 20 mm diametrical range) of 55 mm length (provided by Boston Scientific UK). The rigid Auxetic stent used was 49 mm long, the outer diameter was 13 mm and the wall thickness was 1 mm as shown in Fig. 20. The expansive deformation of the stent upon each pressure increment was then recorded until the point of stent fracture.

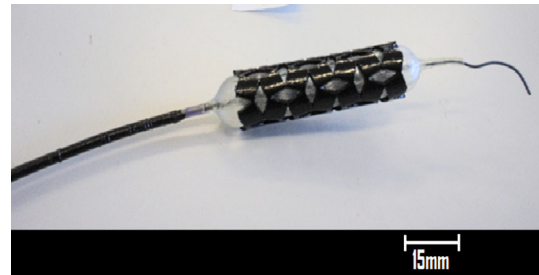


Fig. 20 Rigid Auxetic stent mounted on a balloon catheter

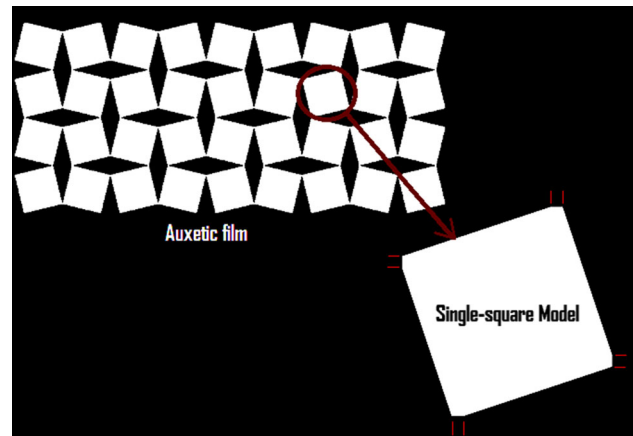


Fig. 21 Single-square FEA model extracted from the Auxetic film

2.6 Finite element analysis

2.6.1 Single-square model

The Single-square FEA model was developed by using ABAQUS 6.10-1 to validate the acquired physical stress–strain (tensile) data and Poisson's ratio values of the Auxetic polyurethane film. The FEA model involved the modelling of a single unit square of the Auxetic (rotating-squares geometry) film. A 3D shell plane-stress model of 500 μ thickness was created, containing the geometry of an Auxetic rotating-square. When designing the unit square part for the FEA model, great attention was given to each detail of a rotating square in the Auxetic film such as; the angle of a rotating square, size and slope of each slit located at each vertex of the rotating square from where it connects to the adjacent squares of the Auxetic film (Fig. 21).

Continuum (CPS8R) 8-node biquadratic plane-stress quadrilateral reduced integration elements were used to model the single unit square as shown in Fig. 22. The elastic–plastic material properties for the single-square model such as Elastic modulus, Poisson's ratio, Yield stress values with relative Plastic strain values, were taken from the physical baseline tensile data of the Polyurethane film (as was described earlier in Sect. 2.5.1). Therefore, the

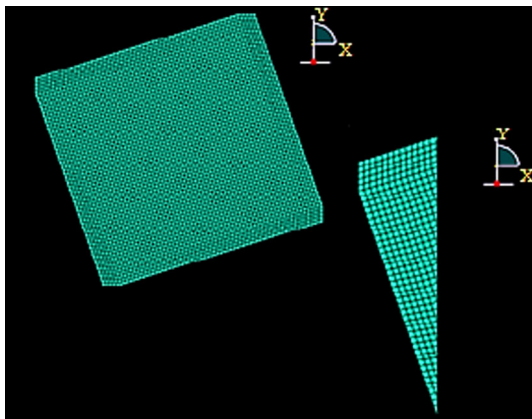


Fig. 22 A single unit square FEA model meshed using quadrilateral elements

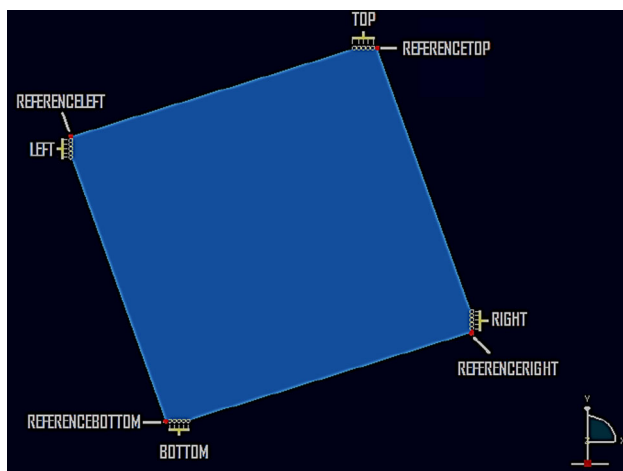


Fig. 23 Two nodesets were created at each vertex of the single-square model

polyurethane material had a Young’s Modulus of 194.3 MPa and a Poisson’s ratio of 0.3 was assigned to the model.

At each slit located at the four vertices of the single-square model, five elements were used. Two nodesets were created at each slit or vertex of the single-square model. First nodeset was created by assigning one node as a reference node of that vertex, and the second nodeset was formed by joining the remaining five nodes of that vertex. Subsequently, the relative names were given to both nodesets at each vertex of the single-square model. The first nodesets were named as; REFERENCELEFT at the upper-left vertex, REFERENCEBOTTOM at the bottom vertex, REFERENCERIGHT at the lower-right vertex and REFERENCE TOP at the upper-right vertex respectively. Similarly, the second nodesets from the upper-left, bottom, lower-right and upper-right vertices of the square were named as LEFT, BOTTOM, RIGHT and TOP respectively (in Fig. 23).

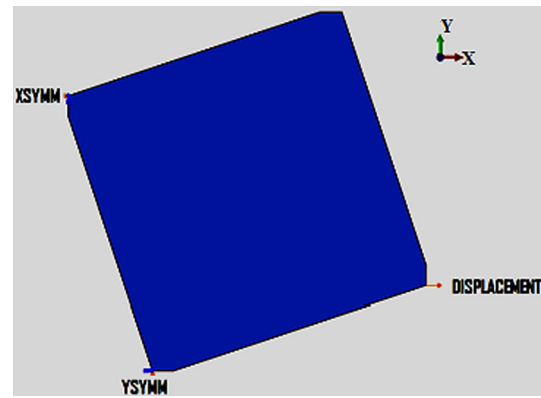


Fig. 24 Boundary conditions applied on the single unit square model

Multiple-point constraints were used to connect the reference nodesets of each vertex to their neighbouring nodesets in the same vertex. Consequently, REFERENCELEFT nodeset was connected to LEFT nodeset, REFERENCEBOTTOM nodeset was joined with the BOTTOM nodeset, REFERENCERIGHT was connected to RIGHT, and REFERENCE TOP was linked up with the TOP nodeset. Then the reference nodesets of all the vertices of the single-square model started controlling the mechanical motion of their neighbouring nodesets, which means that they started controlling the motion of their respective vertices. The symmetry boundary conditions were applied only on the reference nodesets of each vertex of the single-square model. Therefore, the XSYMM (symmetry constraint along x-axis) boundary condition was applied on the REFERENCELEFT nodeset, YSYMM (symmetry constraint along y-axis) was applied on the REFERENCEBOTTOM nodeset, and displacement (U1) in millimetres along x-axis was applied on the REFERENCE RIGHT nodeset as illustrated in Fig. 24.

The mesh convergence test was performed to ensure the accuracy of the finite element model. The convergence test was carried out using different number of elements (mesh densities) or seed sizes. Different reaction force values at REFERENCE RIGHT nodeset were acquired by keeping the value of applied displacement at REFERENCE RIGHT nodeset constant i.e. 0.1 mm. The reaction force values were converged at 4624 number of elements (i.e. 0.05 seed size) and the total CPU time utilised was 90 s.

Consequently, a number of displacement values along x-axis, starting from 0.1 to 6.5 mm, were applied in small increments to the REFERENCE RIGHT nodeset. This led to the beginning of the single-square model rotation, which was relative to the incremental displacement at the REFERENCE RIGHT nodeset. Then the reaction force values at REFERENCE RIGHT nodeset and the displacement values along y-axis at REFERENCE TOP nodeset were recorded. The reaction force values (along x-axis) at the

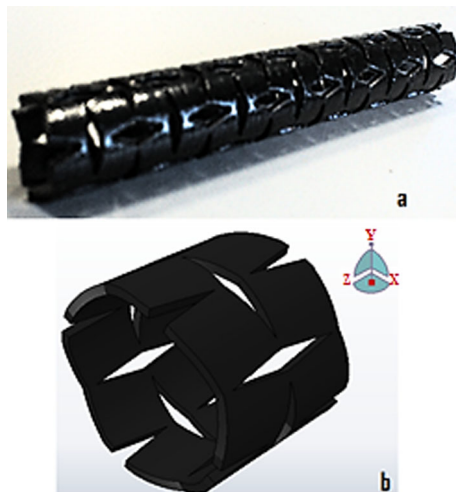


Fig. 25 **a** Rigid Auxetic polyurethane stent, and **b** rigid Auxetic-ring FEA model

REFERENCELEFT and REFERENCERIGHT nodesets were the same, and there was zero reaction force value at REFERENCEBOTTOM and REFERENCETOP nodesets (along both x and y axes).

It was considered that the single-square model behaved rather like a mechanical spring. This framework allowed the real force and displacement behaviour of an Auxetic film consisting of a number of these unit cells in both x and y axes to be calculated. The following formula (in Eq.1) was used to convert the reaction force values of the single-square to the force values of the Auxetic film comprising of number of squares in x and y axes. The number of squares in x and y axes of the Auxetic film, were selected from the gauge length and width of the Auxetic polyurethane film specimen which was physically tensile tested (in earlier Sect. 2.5.1).

$$F = KX$$

Here ‘X’ is the applied displacement along x-axis to the REFERENCERIGHT nodeset, ‘RF’ is the reaction force acquired from the same nodeset and ‘K’ is the stiffness of the single square in Newton per meter.

$$K = \frac{RF}{X}$$

And M_x is the number of squares in longitudinal direction (x-axis), N_y is the number of squares in transverse direction (y-axis)

Therefore, total force of the Auxetic film was derived from the following expression,

$$F_T = \left(K \times \frac{N_y}{M_x} \right) \times (X \times M_x) \quad (1)$$

Finally, both the physical test data and the FEA data derived from the single-square model of the Auxetic

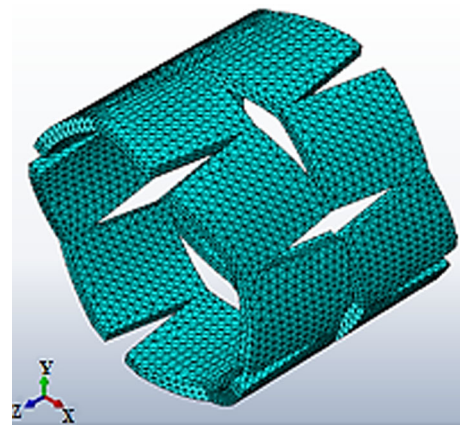


Fig. 26 Auxetic-ring model meshed with tetrahedral elements

polyurethane film were compared at different longitudinal and transverse extension values, and the percentage error was also calculated. The Poisson’s ratios of both physical Auxetic polyurethane film and Auxetic finite element film model, were also calculated and compared at a range of extension values along x and y axes.

2.6.2 Auxetic-ring model

The physical rigid Auxetic oesophageal stent was simulated by creating an Auxetic-ring FEA model. The FEA model was structurally the same as the rigid Auxetic polyurethane stent which was developed by using vacuum casting manufacturing technique. However, it varied in dimensions as the length of the FEA model comprised of only one unit cell (having four rotating-squares). The outer diameter and wall thickness of the FEA model was the same as the physical rigid stent being 13 and 1 mm respectively. The model comprised of only one Auxetic ring in length (in Fig. 25b), since only diametrical changes had to be observed at various radial displacements.

The other difference between the Auxetic-ring model and the physical oesophageal stent being the polyurethane material. Since, the physical Auxetic stent was made of rigid polyurethane material (“PX-212” acquired from Axson UK Ltd.) of 75 shore D hardness. Hence, a different rigid polyurethane material (“Pellethane” supplied by Smith & Nephew UK) of 75 shore D hardness was assigned to the FEA model, which was previously tested physically in the Baseline tensile test (described earlier in Sect. 2.5.1). The elastic–plastic material properties were taken from the Baseline tensile data of this polyurethane, and material properties of 194.3 MPa for the Young’s modulus and 0.3 for the Poisson’s ratio were assigned to the FEA model. Four-node tetrahedral elements were used to mesh the model (Fig. 26), and the total number of elements was 20,800 requiring a total CPU solution time of 9 min.

Fig. 27 **a** An un-deformed Auxetic-ring FEA model, and **(b)** deformed at 1 mm outward radial displacement applied outwardly from the lumen

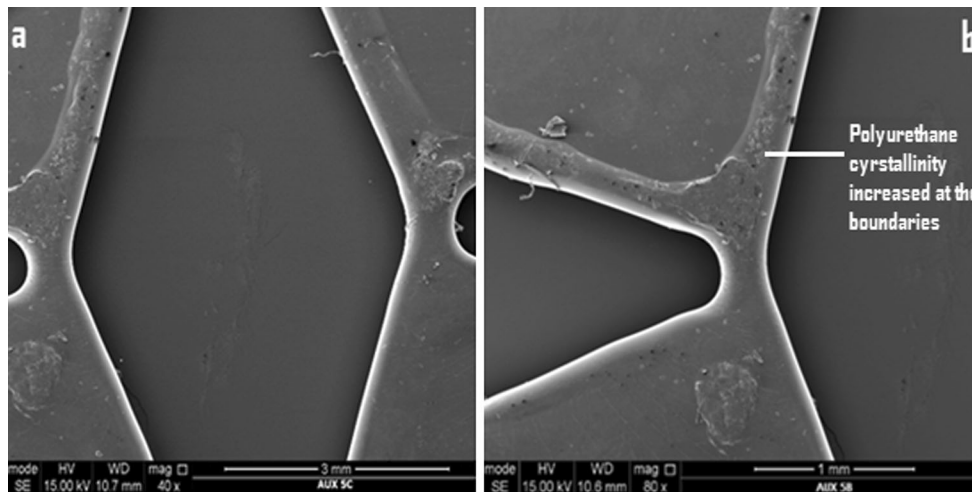
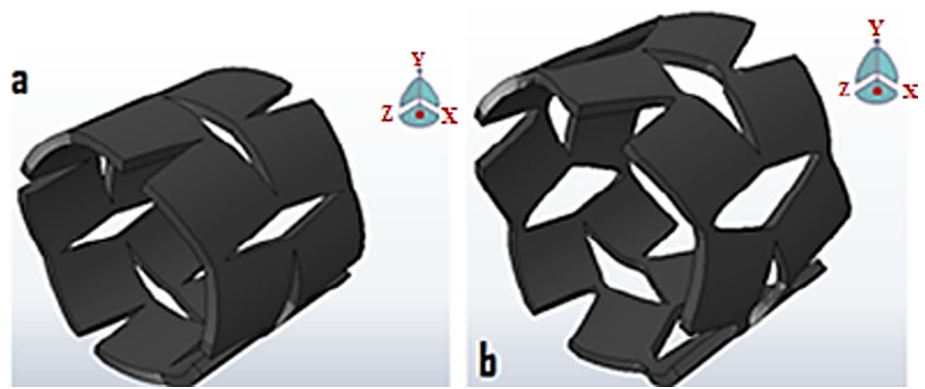


Fig. 28 SEM micrograph of the sample from the lasercut Auxetic polyurethane film, **a** at $\times 40$ magnification, and **b** $\times 80$ magnification

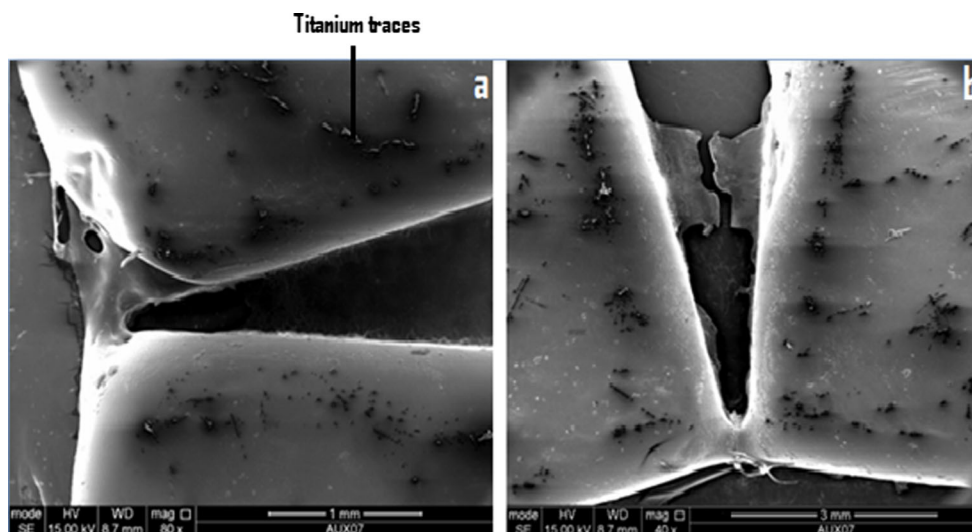


Fig. 29 Micrographs of the second sample at **a** $\times 80$ magnification and **b** $\times 40$ magnification

The Z-SYMM (symmetry constraint along z-axis) boundary condition was applied on the proximal end of the Auxetic-ring model, and the distal end of the model was

free to move only in the x and y axes. A range of outward radial displacement values (in mm) were applied on the lumen of the Auxetic-ring model. The radial reaction force

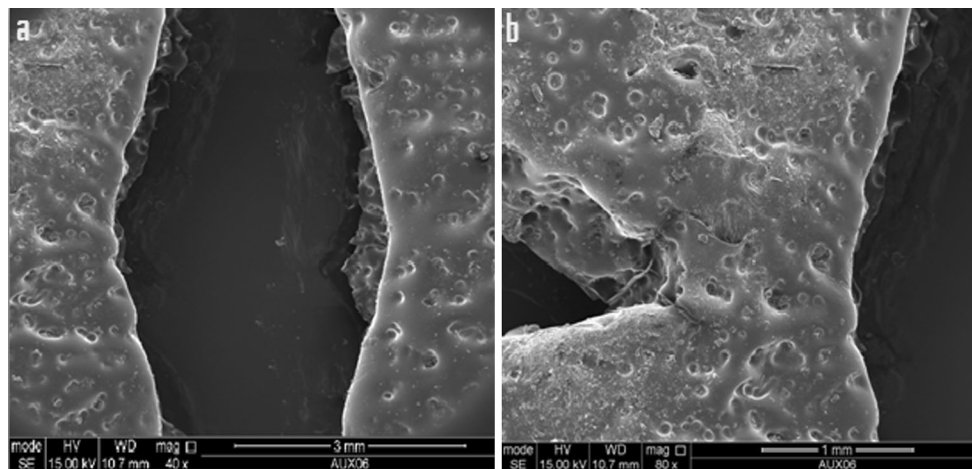
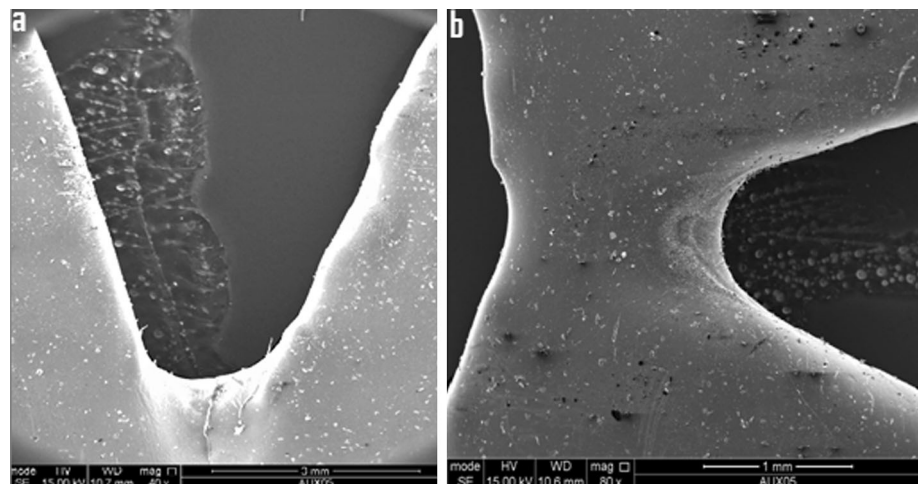


Fig. 30 Micrographs of the sample taken from the Auxetic polyurethane stent made by casting into the titanium alloy collapsible tubular die, **a** at $\times 40$ magnification and **b** at $\times 80$ magnification

Fig. 31 SEM micrographs of the second sample at **a** $\times 40$ magnification and **b** $\times 80$ magnification



values were calculated at different radial displacement values applied to the model from the luminal side. The obtained radial reaction force values were then divided by the area of the Auxetic-ring model so as to calculate the radial pressure values. Finally, the calculated radial pressure values at different applied radial displacement values of the model were then tabulated and compared with the data gathered from the physical stent expansion Test-III (in previous Sect. 2.5.2). Additionally, the stress concentrated areas and weak structures within the radially deformed Auxetic-ring model were identified (Fig. 27).

3 Results and discussion

A manufacturing route which ranged from conventional subtractive techniques to new additive manufacturing techniques was employed for the fabrication of Auxetic oesophageal stents in seamless fashion. Polyurethane was used as a material due to its biocompatibility and non-

toxicity response. Hence in the following section the adopted manufacturing approach will be critically analysed by appraising the efficacy of each method and the quality of the end product.

3.1 Surface characterisation

The SEM was used to characterise the surface morphology of Auxetic (rotating-squares) geometry produced by different manufacturing techniques. This study was actually performed to check the quality of Auxetic unit cells (comprising of four rotating squares) produced by different methods using polyurethane material in both films and tubular (seamless) stent forms.

3.1.1 Auxetic polyurethane films

The purpose of this investigation was to analyse the surface quality of the Auxetic polyurethane films produced by different manufacturing techniques. Therefore, the first

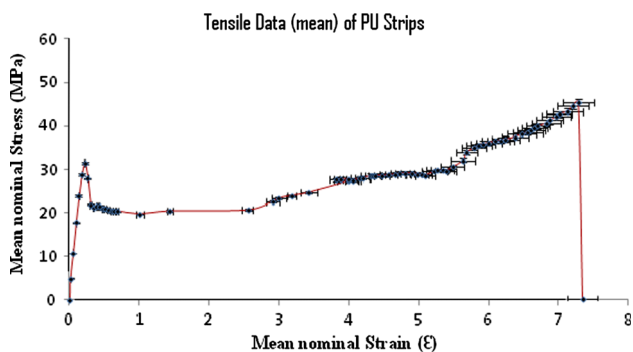


Fig. 32 Nominal (mean) stress–strain data of the polyurethane samples with standard error ($SE = SD/\sqrt{n}$ with x-axis SE range (0.0003–0.23) and y-axis SE range (0–0.81)

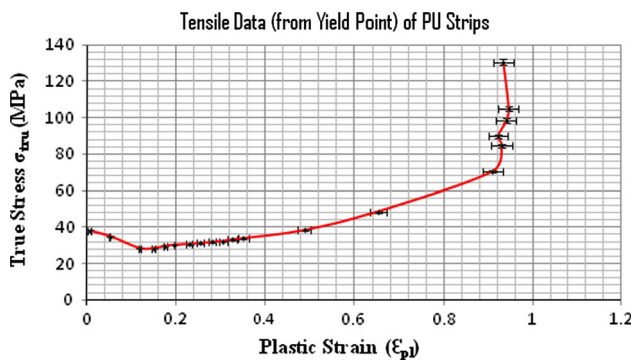


Fig. 33 True stress and Plastic Strain data calculated with standard error ($SE = SD/\sqrt{n}$, x-axis SE range (0.001–0.022) and y-axis SE range (0.2–1.6)

sample was selected from lasercut Auxetic polyurethane film for analysis, and initially it was viewed at 40 and 80 times magnifications (in Fig. 28).

From the above micrographs, it was observed that, the material which was melted by the fine laser beam while cutting was removed effectively by the covering (coaxial gas jet with laser beam) gas out of the diamond-shaped kerf. It was found that, the microscopic softened material, which was not blown away from the cut kerf and resided within the confines of the diamond-shaped cut, densified the boundaries of the squares and hinges located in close proximity. It was established that there were no significant surface irregularities and the edges of the Auxetic unit cell were properly rounded off. Additionally, the edges of both solid squares and their corresponding hinges were found to be densified by lasercutting process, and the densified areas indicated an increase in crystallinity. It is well established fact that thermal treatment of polyurethane, affects the hard segment of the polyurethane, increasing the crystallinity and ultimately increasing the Young’s modulus of polyurethane.

The second sample was acquired from the Auxetic polyurethane film, developed by casting onto a titanium alloy mould. The micrographs demonstrated that, there was

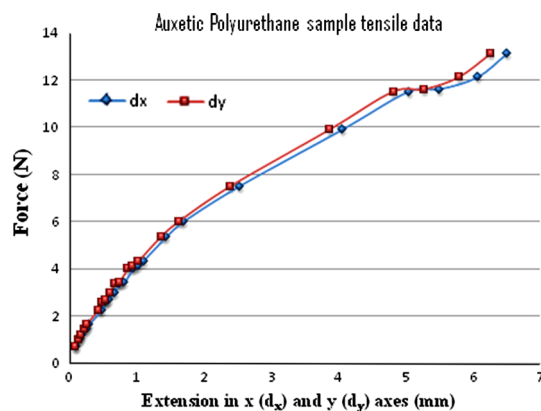


Fig. 34 Tensile data of the Auxetic polyurethane sample acquired from manual calculation at different loads

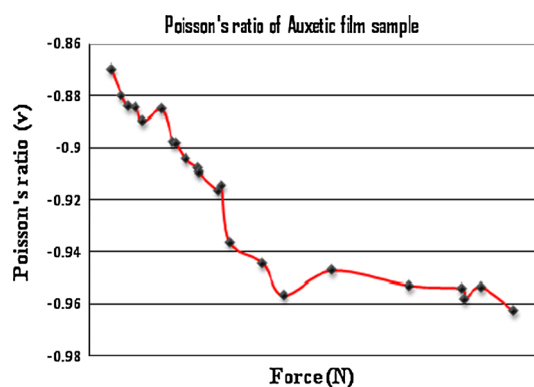


Fig. 35 Poisson’s ratio of the Auxetic polyurethane sample at different loads

some material still remaining within the diamond-shaped cuts as illustrated below in Fig. 29. Since, titanium oxide passive layer was created on the surface of the titanium mould due to the high reactivity of titanium with oxygen in the air. Therefore, a significant amount of black microscopic particles appeared on the surface of the Auxetic polyurethane sample. These small particles were actually titanium traces, which adhered to the polyurethane matrix, and this adhesion has recently been analysed by [15]. It was found that some of the hinges located within the squares of the sample were either cracked or weak. It was also established that there were some surface irregularities and the edges of the sample were rounded off.

It was established from the SEM micrographs that, lasercutting method is an effective and rapid way of producing Auxetic films due to the fact that cutting is the only process step involved in this technique. In addition, this technique not only produced good quality Auxetic polymeric films, but also reinforced those regions (edges and hinges) of the Auxetic (rotating-squares) network which were later found to be weak and more prone to failures. The Auxetic film casted on a titanium reverse-Auxetic mould

was flat and smooth without having surface irregularities or entrapped air bubbles, and the only drawback of this fabrication method was that the titanium traces (microscopic) appeared on the surface of the Auxetic film as shown in Fig. 29 and the process was lengthier than laser cutting.

3.1.2 Auxetic oesophageal stents

The quality of the rotating-squares geometry of the Auxetic stents produced by different manufacturing techniques was examined by using SEM micro images. Consequently, the sample of the Auxetic unitcell (comprising of four rotating squares) was selected from the seamless Auxetic polyurethane stent made by casting the pre-degassed polyurethane resin into the collapsible tubular mould made of titanium alloy. The sample was viewed at 40 and 80 times magnifications (in Fig. 30).

The micrographs in Fig. 30 visibly demonstrate that, due to the rough granulated surface of the collapsible tubular mould made of titanium alloy, a significant amount of small dents were present on the surface of the Auxetic stent sample. It was also found that the edges

were sharp and irregular and the surface irregularities were quite high.

The next sample was taken from the seamless Auxetic polyurethane stent produced by vacuum casting technique, and it was viewed at 40 and 80 times magnifications (in Fig. 31).

From the micrographs presented in Fig. 31, it was observed that the surface quality of the Auxetic sample was good without having any irregularities. It was also found that the edges of the Auxetic unitcell were properly rounded off.

The quality of the seamed Auxetic stent which was developed by configuring the lasercut Auxetic film into tubular stent form, was good with only one disadvantage of having welded joints (which would be more susceptible to mechanical failures). It is envisaged that by lasercutting seamless polyurethane tubes instead of films would not only avoid the problem of having welded joints but also the production time would be reduced significantly. The vacuum casting technique was found to be simple but the process time was much longer than the laser cutting method. The Mastermodel and silicone mould can be used number of times in vacuum casting method, and it is

Fig. 36 Graph of the Auxetic polyurethane film sample plotted by the tensile tester, **a** load versus extension, **b** stress versus strain (%) and **c** undeformed and plastically deformed Auxetic polyurethane film

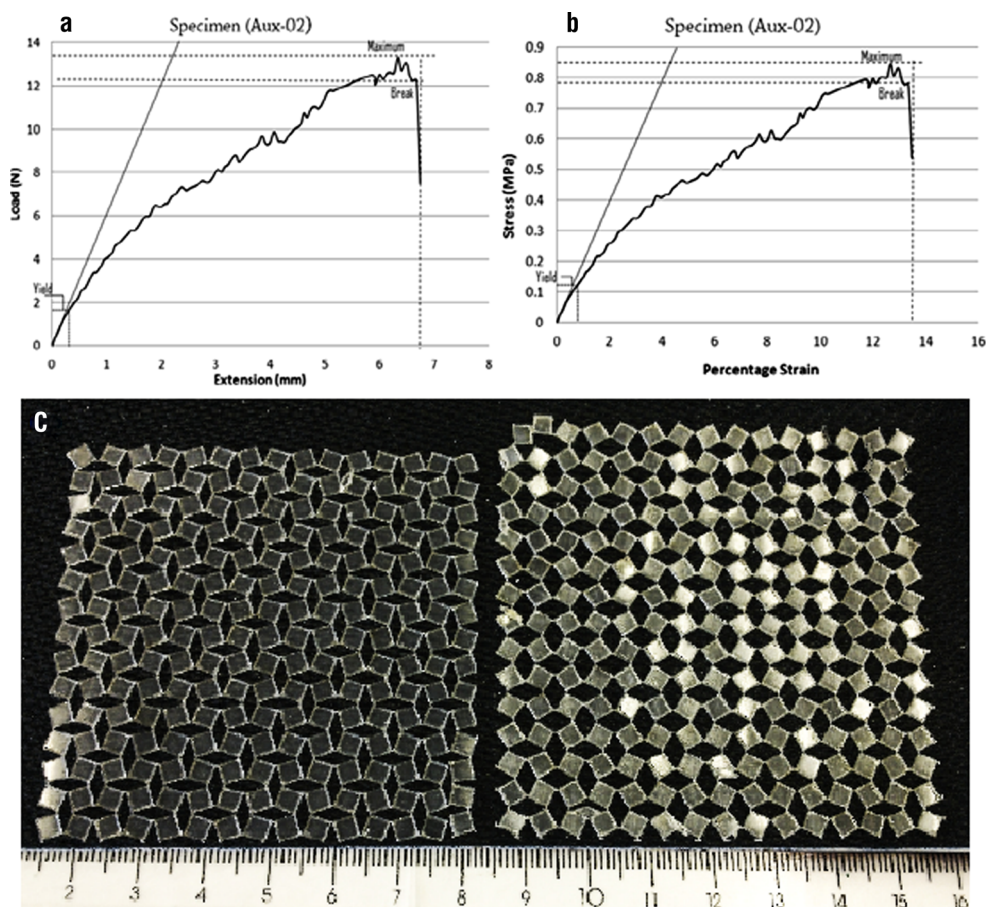


Table 1 Semi-rigid Auxetic oesophageal stent expanded by the balloon catheter

Pressure (bar) from balloon	Stent diameter (mm)	Stent length (mm)
0.0	10.00	50.00
0.5	10.50	50.15
0.8	10.78	50.56
1.0	11.50	51.22
1.5	12.12	51.70
1.7	12.65	51.70
2.0	13.73	51.80
2.5	15.44	51.81
2.7	15.73	51.83

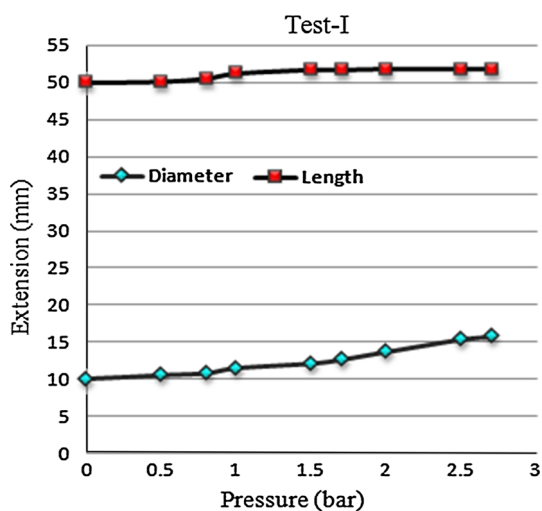


Fig. 37 Graph showing diametrical and length changes of the Auxetic Oesophageal stent

therefore a one-off investment. The Auxetic oesophageal stents produced by this technique were of good quality.

3.2 Tensile test data

3.2.1 Mechanical behaviour of Auxetic polyurethane films

The lasercut Auxetic polyurethane films were selected for mechanical testing because of the comparatively good quality of the Auxetic films. In the beginning, the baseline tensile data was acquired by testing the same rigid polyurethane films used in the fabrication of the Auxetic polyurethane films by lasercutting technique. The gauge length and width of the 0.5 mm thick polyurethane strip sample were 50 and 20 mm respectively. An experiment was performed by subjecting the polyurethane strip to uniaxial tensile loads, and nominal stress–strain (baseline) data was gathered. The mean of the nominal tensile

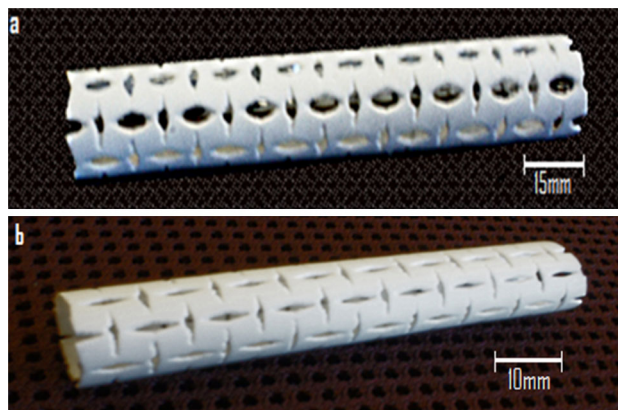


Fig. 38 Auxetic Oesophageal stent expanded by the balloon catheter, **a** a plastically deformed (expanded) stent and **b** an un-expanded Auxetic stent

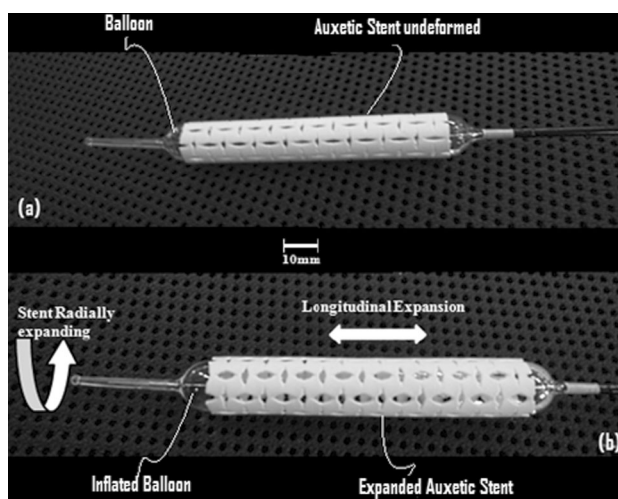


Fig. 39 Semi-flexible Auxetic stent tested by the small diameter balloon catheter, **a** Auxetic stent mounted on a balloon catheter and **b** expanded Auxetic stent (both in radial and longitudinal directions)

(baseline) data from different samples was subsequently taken as illustrated in Fig. 32. The graph in Fig. 32 clearly shows that the polyurethane sample was yielded at a nominal (mean) stress of 31.4 MPa to a maximum of 22.17 % (mean) strain at 5.33 mm extension. The elastic modulus of the polyurethane sample was calculated as 194.3 MPa.

The nominal tensile stress–strain data was then converted into True stress and Plastic strain data, which was later used as material (elastic–plastic) data for finite element models as shown below in Fig. 33.

A tensile test of the Auxetic polyurethane sample was carried out (as mentioned previously in Sect. 2.5.1), after the baseline tensile data of the polyurethane material was obtained. This test was performed manually as both longitudinal and transverse extension values of the Auxetic

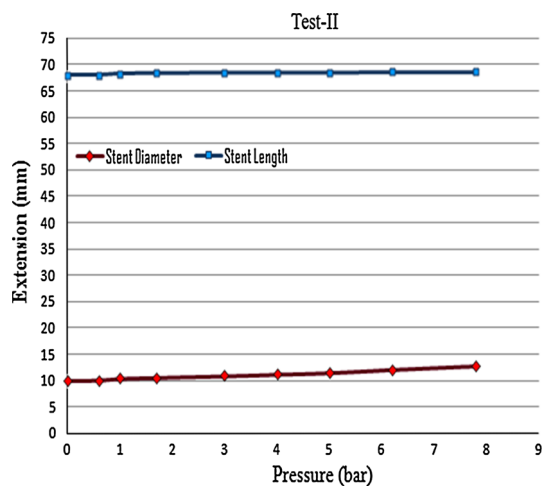


Fig. 40 A graph showing radial and longitudinal expansion of the stent at different pressure increments

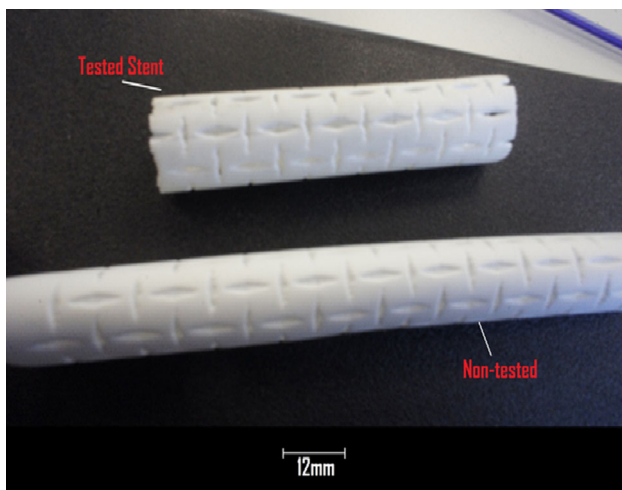


Fig. 41 Oesophageal stent exhibiting a slight change in size, after removing from the balloon in Test-II

sample were calculated at different uniaxial tensile load increments till the point of sample's failure (in Fig. 34).

The gauge length and width of the above 0.5 mm thick Auxetic polyurethane sample were 50 and 31.5 mm respectively. The Poisson's ratio of the Auxetic sample was also calculated, which ranged from 0.87 to 0.963 at different load values as illustrated in Fig. 35.

In another investigation the tensile test of the Auxetic polyurethane sample was carried out automatically by the tensile testing equipment until the point of sample's failure. It is clearly shown in the graph created by the software of the tensile tester in Fig. 36a, b. The sample yielded at a tensile load of 1.8 N which is a stress of 0.135 MPa to a maximum 0.95 % strain and at 0.38 mm extension. The Auxetic sample finally failed at 12.2 N of force at a maximum 13.62 % strain and at 6.67 mm extension (in

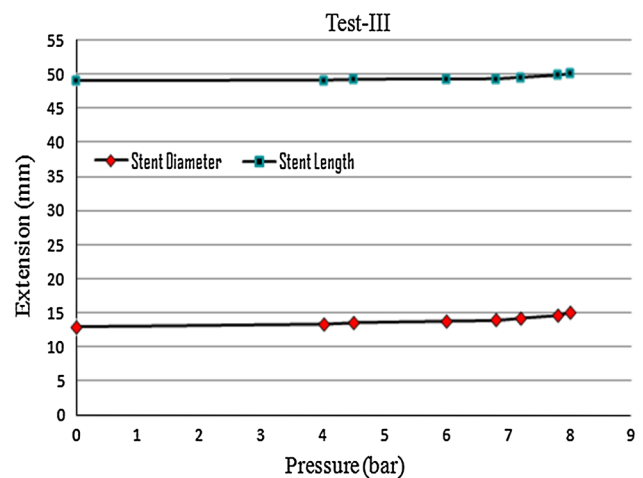


Fig. 42 Expansion data of the rigid Oesophageal stent

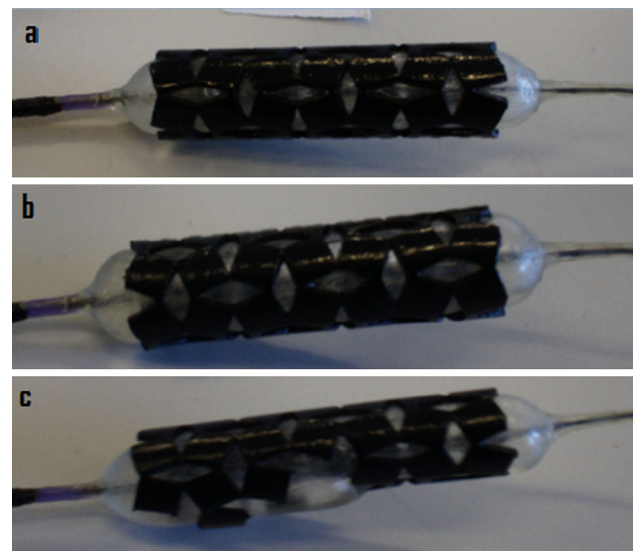


Fig. 43 a An un-expanded rigid Auxetic Oesophageal stent, b an Auxetic stent radially expanded 1.8 mm at 7.85 bar pressure, c the stent finally broke at 8.3 bar pressure

Fig. 36a, b). It was observed after removing the sample from the testing equipment that the Auxetic polyurethane sample was plastically permanently deformed. It was found from the SEM surface morphology analysis of the Auxetic polyurethane film fabricated by lasercutting technique that, the edges of both solid squares and their corresponding hinges were densified, which indicated an increase in crystallinity. It is a well-established fact that the thermal treatment of polyurethane, affects the hard segment of the polyurethane, which increases crystallinity, ultimately increasing its Young's modulus. Therefore, it was established during tensile testing of Auxetic film sample that the densified edges of the solid squares and their corresponding hinges allowed the sample to withstand a significant amount of stress until the point of failure. These edges

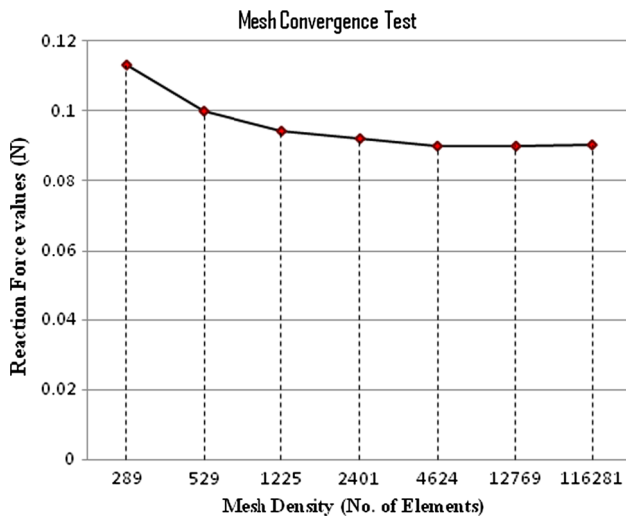


Fig. 44 Graph showing Reaction force values collected at different Mesh densities

were later found to be the stress concentrated (weak) areas in the Auxetic rotating squares geometry (in Sect. 3.2.2).

It was also established that the diamond-shaped spaces (hollow) between rotating squares played a crucial role in the overall expansion of the Auxetic film. The Auxetic film containing wide diamond-shaped spaces between the rotating-squares. In effect as the squares became more angulated they expanded less, as there was less room left for the rotation of their neighbouring squares. Similarly, the Auxetic film having narrow diamond-shaped spaces (i.e. the squares were less angulated), allowed the neighbouring squares to rotate more, and hence, the Auxetic film expanded more. This was also derived in the analytical model reported previously by [11, 16], describing the mechanical behaviour of the Auxetic (rotating-square) geometry and it demonstrates that the mechanical properties depend on both the relative magnitude of the stretching and hinging constants. The precise square dimensions and the angle between the squares control the value of Poisson’s ratio.

3.2.2 Auxetic oesophageal stents expansion data

It was envisaged that the deployment of the Auxetic oesophageal stent will be without a dedicated expensive delivery system. This will be administered orally into the oesophagus using a significantly small diameter Auxetic stent mounted on a balloon dilatational catheter. The balloon dilatational catheter has already been in use for the pre-dilation of the oesophageal lumen and for the post-dilation of the commercial oesophageal stents. Therefore, a number of tests were performed in this investigation by expanding the seamless semi-rigid and rigid Auxetic oesophageal stents made of polyurethane material, using

Table 2 Reaction force values acquired from “REFERENCE-RIGHT” nodeset at different mesh densities

Seed size	No. of elements	Total CPU time	Reaction force (N)
0.2	289	30 s	0.113099
0.15	529	35 s	0.099976
0.1	1,225	40 s	0.094433
0.07	2,401	1.0 min	0.091966
0.05	4,624	1.5 min	0.090276
0.03	12,769	2.0 min	0.090081
0.01	116,281	6.0 min	0.091303

different sizes of balloon dilatational catheters. The tests were conducted in order to estimate the diametrical change and longitudinal expansion of the stents at different applied radial pressures, and to also check that at which pressure the stent deformed plastically (permanently) without any recoil. The experiment was initially performed (i.e. Test-I) to investigate the mechanical behaviour of a semi-flexible Auxetic oesophageal stent of 50 mm length, 10 mm outer diameter and 0.5 mm wall thickness.

From the Table 1 and in Fig. 37, it was found that the oesophageal stent radially expanded from 0.5 to 5.73 mm and longitudinally extended from 0.15 to 1.83 mm at a range of pressure increments from 0.5 to 2.7 bar applied by the balloon. The oesophageal stent was subsequently removed from the balloon, and the diameter and length of the stent were calculated as 14.94 and 51.8 mm respectively. This clearly showed that the Auxetic stent plastically (permanently) deformed at 2.7 bar pressure and it retracted slightly when removed from the inflating balloon (in Fig. 38). The stent was then mounted again on the balloon catheter and the pressure was applied until the point of stent failure, and the Auxetic oesophageal stent finally broke at a pressure of 2.86 bar.

In Test-II, an experiment was conducted to investigate again the semi-flexible Auxetic stent at different radial pressures applied by the balloon catheter (as mentioned earlier in Sect. 2.5.2). The procedure of this experiment was similar to Test-I, however, the specifications were changed as different stent length (i.e. 68 mm) and size of the balloon catheter (i.e. 10, 11 and 12 mm diametrical range) were used (in Fig. 39).

From the test data illustrated in Fig. 40, it was found that the oesophageal stent radially expanded from 0.1 to 2.8 mm and longitudinally it extended from 0 to 0.6 mm at pressure increments ranging from 0.6 to 7.8 bar applied by the balloon catheter. Since the radial size of the balloon was smaller, the same radial and longitudinal displacements of the stent (which were acquired in Test-I) required significantly higher inflation pressures.

The test was finally stopped at a pressure of 7.8 bar to avoid exceeding the maximum inflation pressure of the balloon. Hence, due to the small radial size of the balloon, the balloon did not manage to fully expand the stent and to establish reasonable plastic deformation in the stent (in Fig. 41).

A rigid Auxetic oesophageal stent was examined in Test-III, in which radial and longitudinal expansions of the stent were calculated at a range of radial pressures applied from the balloon catheter. The graph in Fig. 42 clearly shows that, the rigid oesophageal stent radially expanded from 0.4 to 2.2 mm and longitudinally extended from 0.1 to 1.14 mm at pressure increments ranging from 4 to 8 bar. The Auxetic stent was finally cracked at 8.3 bar pressure as shown in Fig. 43c.

It was established from the stent expansion tests using semi-rigid and rigid Auxetic stents that, semi-rigid Auxetic stent tend to expand (both radially and longitudinally) more

than the rigid Auxetic stent. This is due to several reasons including (i) the rigid Auxetic stent was too stiff and failed early (at small pressure increments), (ii) there were more squares with their associated plastic hinges (i.e. eight squares or hinges) present circumferentially in semi-rigid Auxetic stent than in the rigid Auxetic stent (which had fewer six squares or hinges circumferentially), (iii) the diamond-shaped (hollow) spaces of the semi-rigid stent were narrow (i.e.1 mm wide) than the spaces in rigid stent (which were 2 mm wide) and (iv) edges of the solid squares and their corresponding hinges were found to be the stress concentrated (weak) areas. It is clearly established from the above tests that the more flexible and thicker the edges of the solid squares and their corresponding hinges are then the greater the stress the Auxetic rotating-squares can withstand. It was also found from this study that the rotation or hinging mechanism of the individual units and their size or angle, played a vital role in

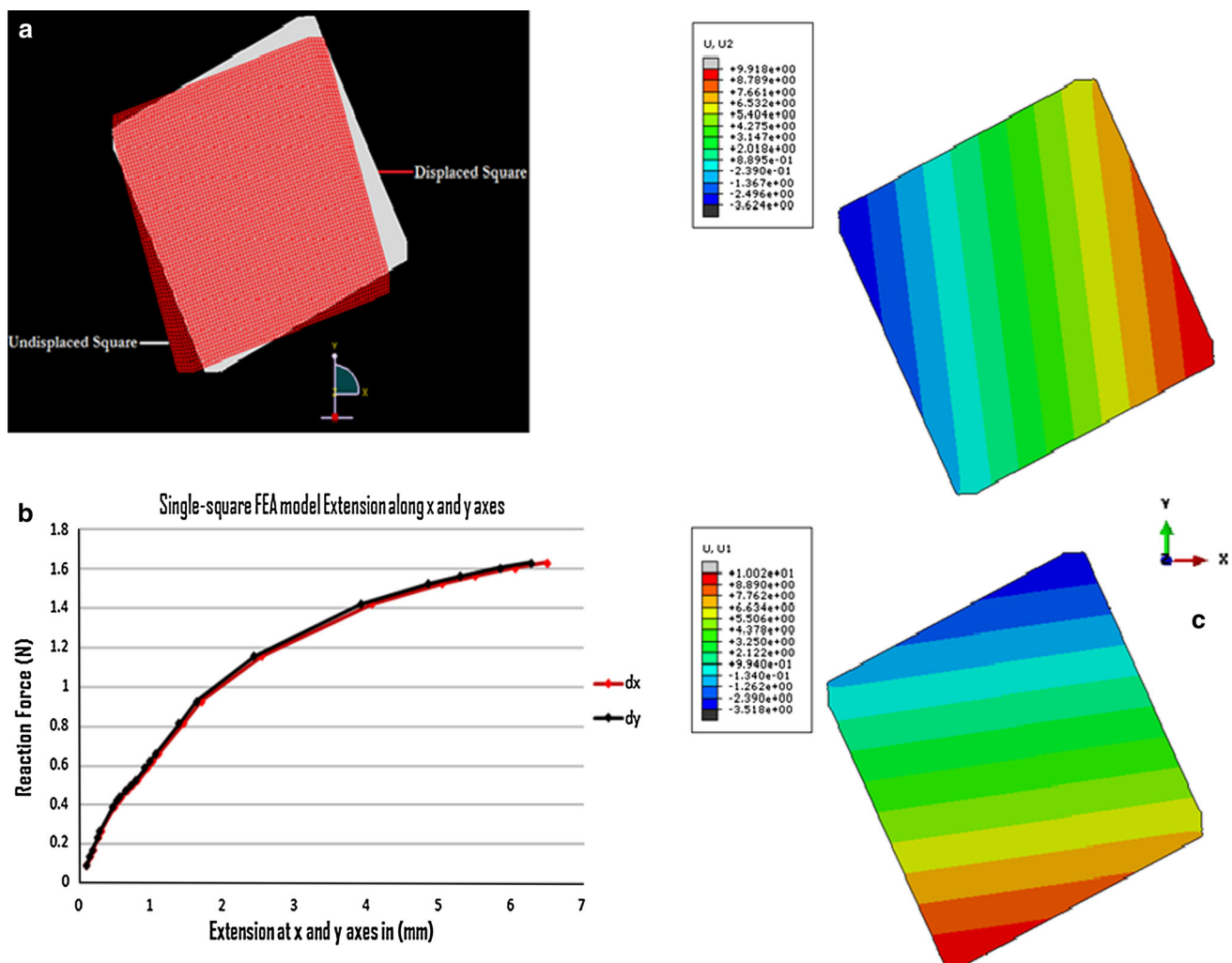


Fig. 45 **a** Rotation of the single-square unit model, **b** a graph showing extension of the model at both x and y axes at different reaction force values, and **c** displacement contours along both x-axis ($U1$) and y axes ($U2$), exhibiting rotation of the single-square model

Table 3 Single-square FEA model displacement along x and y axes at different force values

Reaction force at “ReferenceRIGHT” nodeset (N)	Longitudinal extension (d_x) ^b	Transverse extension (d_y) ^c
0.0899	0.10	0.090
0.1349	0.15	0.138
0.1708	0.19	0.177
0.2338	0.26	0.243
0.2683 ^a	0.30	0.283
0.3877	0.48	0.455
0.4199	0.54	0.510
0.4420	0.59	0.559
0.4742	0.67	0.636
0.4982	0.74	0.705
0.5268	0.81	0.773
0.5890	0.95	0.909
0.6236	1.02	0.976
0.6613	1.10	1.050
0.8171	1.44	1.383
0.9297	1.70	1.630
1.1607	2.53	2.426
1.4248	4.06	3.908
1.5317	5.04	4.850
1.5686	5.50	5.295
1.6109	6.06	5.840
1.6376	6.50	6.280

^a Reaction force value from where the analysis became non-linear
^b Applied displacement at “ReferenceRIGHT” nodeset (along x-axis)
^c Transverse displacement obtained from “ReferenceTOP” nodeset (along y-axis)

the overall expansion of the Auxetic (rotating-squares) network. This was also determined by [11, 12] in their analytical model which showed that the number of individual units (their size and angle) in Auxetic (rotating-square) geometry controls the mechanical behaviour of the Auxetic network and the subsequent Poisson’s ratio.

3.3 Auxetic film modelling data

The single-square FEA model involved one square extracted from the Auxetic (rotating-squares) film. Instead of modelling a complex anisotropic Auxetic film (comprised of a number of rotating-squares in both x and y axes), a novel single-square finite element model was developed in order to simplify the modelling technique and to obtain accurate results. The mesh convergence test was performed initially to ensure the accuracy of the results acquired from the finite element model. The convergence test was carried out by obtaining the reaction force values

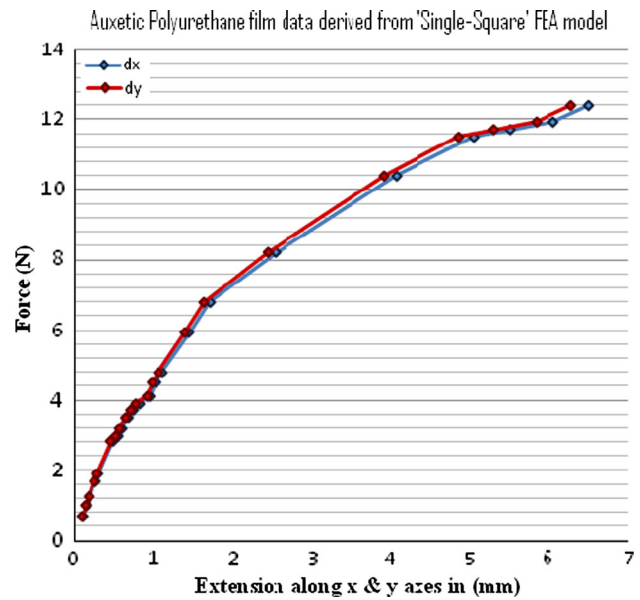


Fig. 46 Auxetic film (extension) modelling data derived from ‘Single-unit square’ FEA model

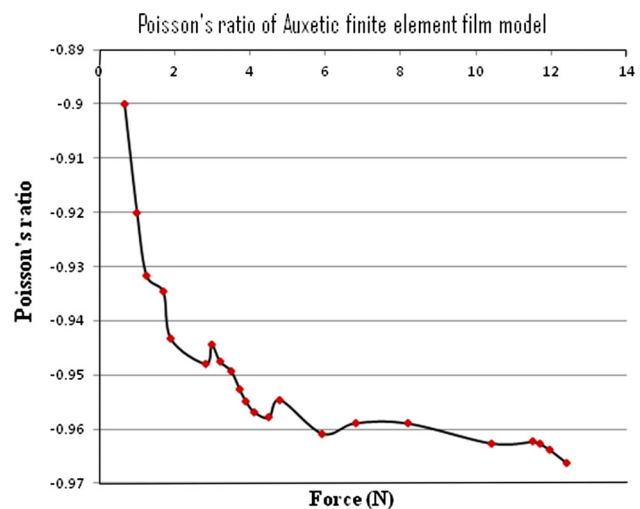


Fig. 47 Poisson’s ratio values calculated from the Auxetic film model (derived from Singleunit square model)

at REFERENCERIGHT nodeset at constant 0.1 mm displacement applied on the same REFERENCERIGHT nodeset. The acquired reaction force values were then plotted against different number of elements (i.e. mesh densities) employed in the model. From the graph in Fig. 44, it is quite clear that the reaction force values were converged at 4,624 number of elements (i.e. at 0.05 seed size), and the total CPU time required to solve the model was just 90 s (Table 2).

The symmetric rotation of the single-square model was generated (in Fig. 45a) by simulating the actual mechanical behaviour of a physical square in an Auxetic (rotating-

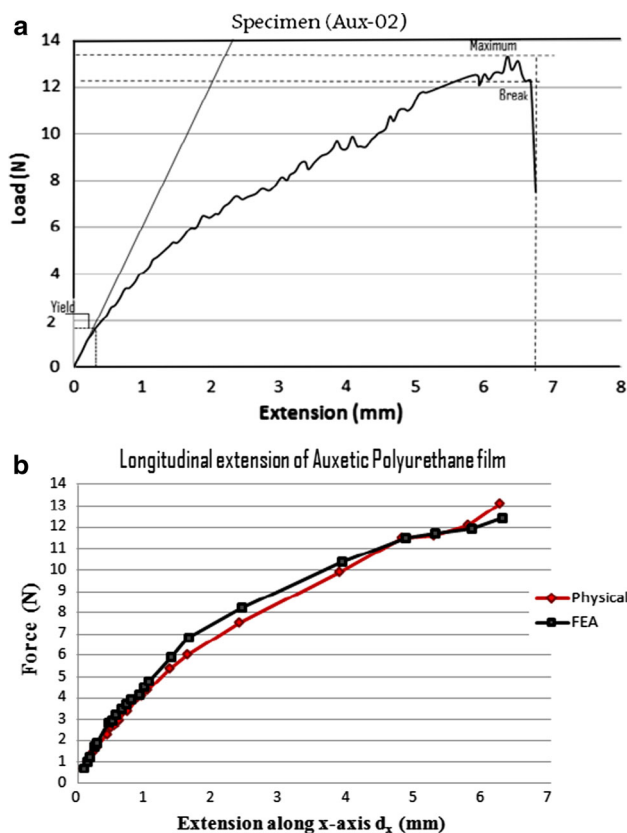


Fig. 48 **a** Automatically calculated tensile data of the Auxetic film from the tensile tester, **b** manually calculated physical data versus FEA modelling data

Table 4 Comparison of physical tensile tests and Auxetic film FEA model data

Auxetic polyurethane film			
	Tensile test (manual)	Tensile test (automatic)	FEA modelling
Load (when yielded)	2.1 N	1.85 N	1.9 N
Extension along x-axis (when yielded)	0.4 mm	0.35 mm	0.3 mm

squares) geometry. Therefore, different displacement values were applied to the REFERENCERIGHT nodeset along x-axis in small increments ranging from 0.1 to 6.5 mm. The reaction force values were then checked at all the REFERENCE nodesets (along both the x and y axes). It was found that the reaction force values at both REFERENCERIGHT and REFERENCELEFT nodesets along x-axis were non-zero and the same, and the reaction forces at REFERENCEBOTTOM and REFERENCE TOP nodesets were found to be zero. The displacement values at REFERENCE TOP nodeset were recorded along the y-axis at every small increment of the displacement applied to the REFERENCERIGHT nodeset along x-axis (in Table 3).

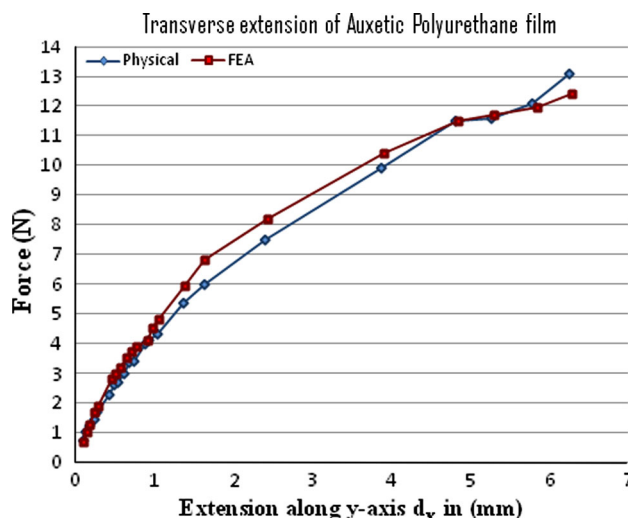


Fig. 49 A graph showing extensions of the physical Auxetic film and Auxetic film (FEA) model along y-axis

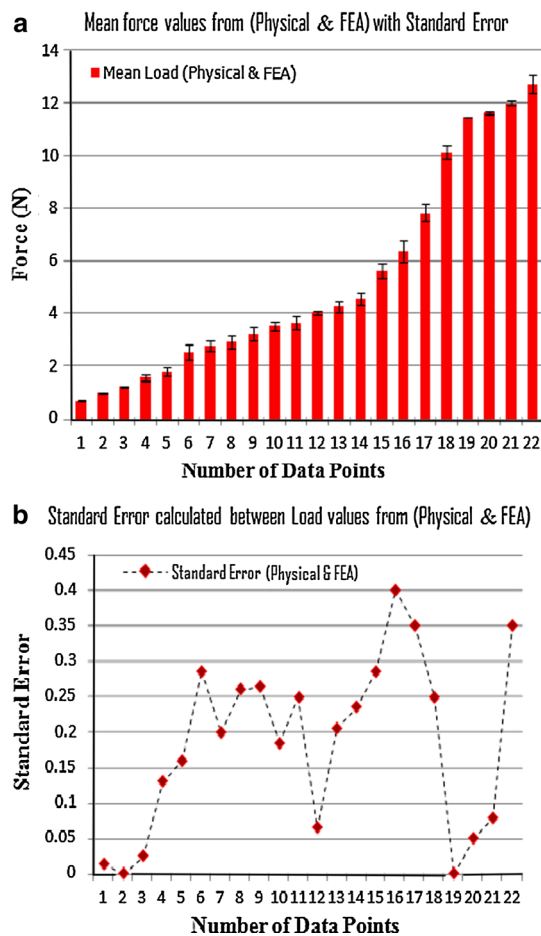


Fig. 50 **a** Graph showing mean load values which were taken from the physical test and FEA model. **b** A graph showing SE between the physical and FEA load values

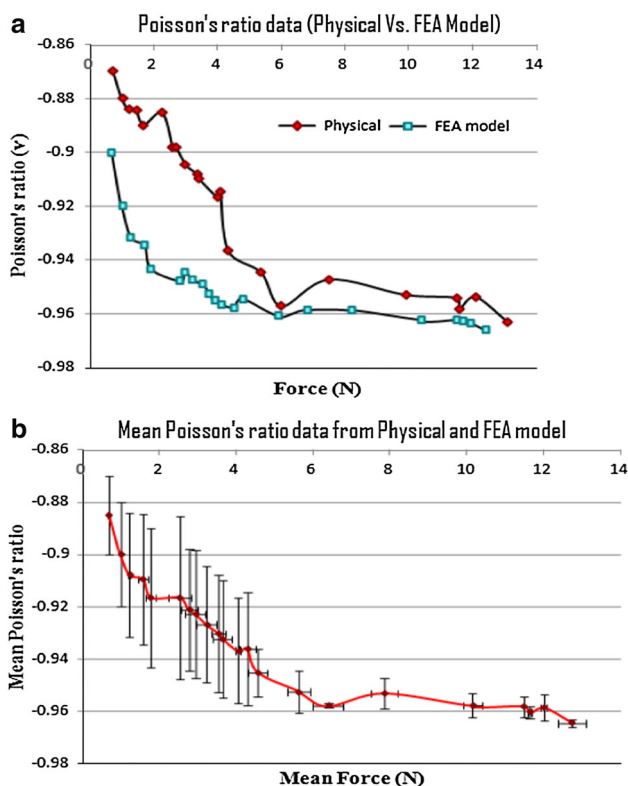


Fig. 51 **a** A graph showing Poisson's ratio values taken from both physical Auxetic film and FEA model at different loads, and **b** Mean Poisson's ratio and load values calculated with Standard Error (SE = SD/ \sqrt{n} , x-axis SE range (0–0.4) and y-axis SE range (0.0008–0.03))

The rotation of the single-square model was estimated by arranging both horizontal displacement (i.e. applied displacement in small increments to REFERENCERIGHT nodeset along x-axis) and vertical displacement (calculated displacement values at REFERENCETOP nodeset along y-axis) with a range of reaction force values obtained from REFERENCERIGHT nodeset as shown below in Fig. 45b. The vertical and horizontal displacement contours of the single-square model as shown in Fig. 45c, visibly demonstrated the rotation of the model.

The Eq. 1 in the previous Sect. 2.6.1, was subsequently used to convert all the above reaction force values of the single-square model into the force values of the Auxetic polyurethane film (having number of squares in x and y axes). The number of squares in x and y axes of the Auxetic film were selected from the gauge length and width of the Auxetic polyurethane film specimen which was previously tensile tested (in the earlier Sect. 2.5.1). The number of squares were selected as $M_x = 11.8$ in x-direction and $N_y = 7.4$ in y-direction. Consequently, a range of force values of the Auxetic polyurethane film (comprising of a known number of squares in x and y axes) were derived at a range of displacement values along both x and y axes as shown in Fig. 46.

The Poisson's ratio values of the Auxetic film model were also calculated ranging from -0.9 to -0.96 at a range of displacement (extension) values of the model along both x and y axes as illustrated below in Fig. 47.

3.3.1 Physical versus finite element modelling results

In this analysis, the physical tensile data of the Auxetic polyurethane films obtained from both manual calculations and from the data automatically generated by the tensile tester as shown in the previous Figs. 34 and 36a, was compared with the finite element modelling results of the Auxetic polyurethane film model (derived from single unit square model). The dimensions of the Auxetic polyurethane film, which was physically tested and the Auxetic polyurethane film that was derived from single-square FEA model were the same.

The graph in Fig. 48b showed that, the physical Auxetic film when tested manually yielded at a load of 2.1 N with an extension of 0.4 mm along the x-axis and which failed at tensile load of 13.1 N which was at a maximum extension of 6.5 mm. When the physical Auxetic film was subjected to a tensile loading and calculations were made automatically by the testing equipment the sample yielded at 1.85 N with 0.35 mm extension along the x-axis and it broke at a force of 12.26 N at a maximum extension of 6.7 mm as shown in Fig. 48a.

Similarly, Fig. 48b shows that, the graph of the Auxetic film (FEA) model became non-linear at a load of 1.9 N at an extension of 0.3 mm along x-axis, which clearly demonstrated that the model yielded at this load. Table 4 shows a direct comparison between the physical (tensile tests) and FEA modelling results related to the yielding of the Auxetic polyurethane film. It is worth noticing that the agreement between the physical and FEA model results is excellent.

Additionally, the chord stiffness of the finite element model dropped significantly from 6.8 to 1.9 N/mm at displacement values of 0.1–6.5 mm respectively. The decrease in stiffness of the Auxetic film FEA model shows that the hinge region in the model is plastically deformed at 12.4 N force. The physical Auxetic film and FEA model also both extended in transverse direction (along y-axis) because of the negative Poisson's ratio ($-v$) as shown below in Fig. 49.

The longitudinal extension values in the manual tensile data of the Auxetic film and the displacement values applied to the finite element model were very similar. Therefore, the load values calculated in both physical (manual) tensile test of the Auxetic film and a range of reaction force values obtained from finite element Auxetic film model, were subsequently used to calculate the SE between the physical and FEA load values (in Fig. 50).

Fig. 52 **a** Von Mises stress of the FEA model when 0.3 mm displacement was applied at the REFERENCERIGHT nodeset of the model, **b** equivalent and in-plane principal plastic strains were taken at the Yield point of the model

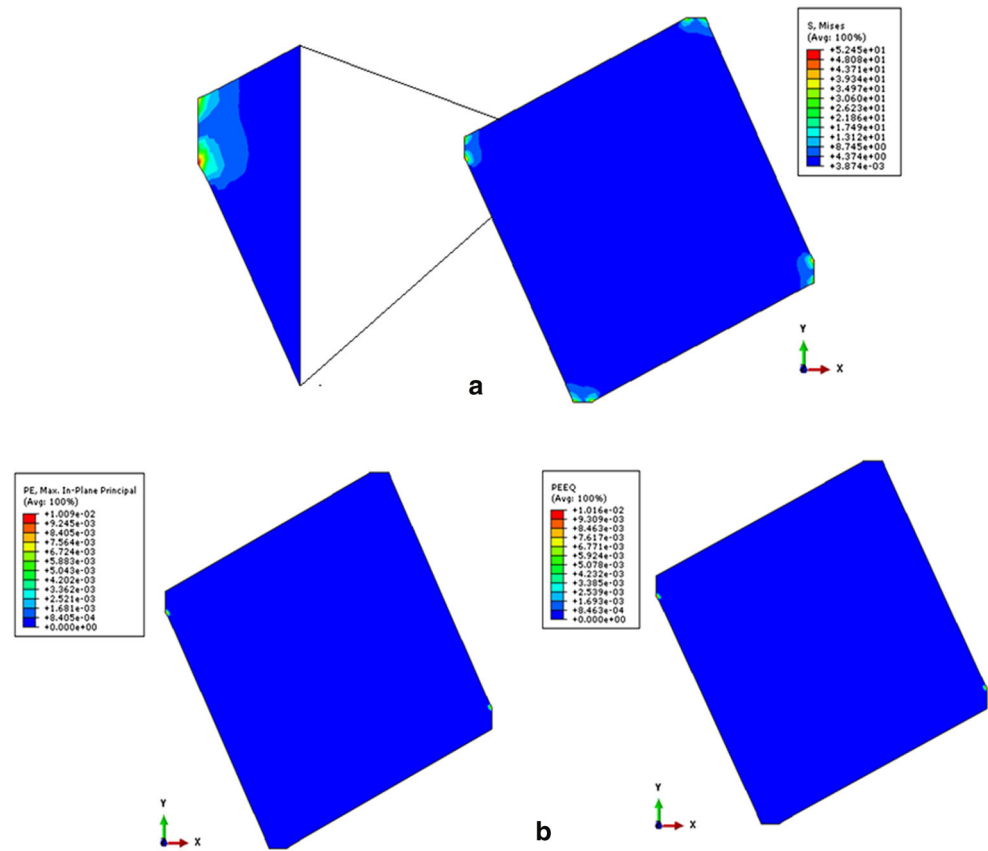


Fig. 53 **a** Auxetic Oesophageal Stent (physical), **b** Auxetic-ring FEA model

The Poisson's ratio values calculated earlier (in the previous Sects. 3.2.1 and 3.3) for both physical Auxetic film and FEA model at different loads, were compared and plotted together as shown in Fig. 51a. A set of mean Poisson's ratio and load values were taken from the Poisson's ratio data (from both physical Auxetic film and FEA model), and the SE was also calculated (in Fig. 51b). It is quite obvious from the comparison that the Poisson's ratio measured and predicted using the FEA was very good.

From the previous graphs in Fig. 36, it was established that the Auxetic polyurethane film when tested by applying

uniaxial tensile loads yielded at an extension of 0.35 mm along x-axis at a maximum 1 % plastic strain (i.e. 0.01 plastic strain). Hence, the Auxetic film FEA model which was derived from the single-square FEA model was carefully analysed under the same conditions.

As it was mentioned earlier in Table 4 that, FEA model became non-linear when 0.3 mm displacement along x-axis applied to the FEA (Auxetic film) model. Therefore, it was noticed that when 0.3 mm displacement (extension) applied to the FEA model along x-axis, the maximum Von Mises stress was found to be 52 MPa, which was significantly greater than the yield strength (set at 38 MPa) of the polyurethane material, and the equivalent plastic strain (PEEQ) and in-plane principal plastic strains (PE) reported in the contour legend were 0.01 (indicating a maximum plastic strain of about 1 %). This clearly demonstrates that the physical Auxetic film and FEA model yielded at 0.35 mm and 0.3 mm extensions (along x-axis) respectively, and the plastic strain values of both physical Auxetic film and FEA model were very similar at the time of yielding as shown in Fig. 52.

3.4 Modelling of the Auxetic oesophageal stent

The rigid Auxetic oesophageal stent used earlier in stent expansion Test-III was simulated by an Auxetic-ring finite

Fig. 54 Radial displacement applied outwardly from the luminal side of the Auxetic stent model

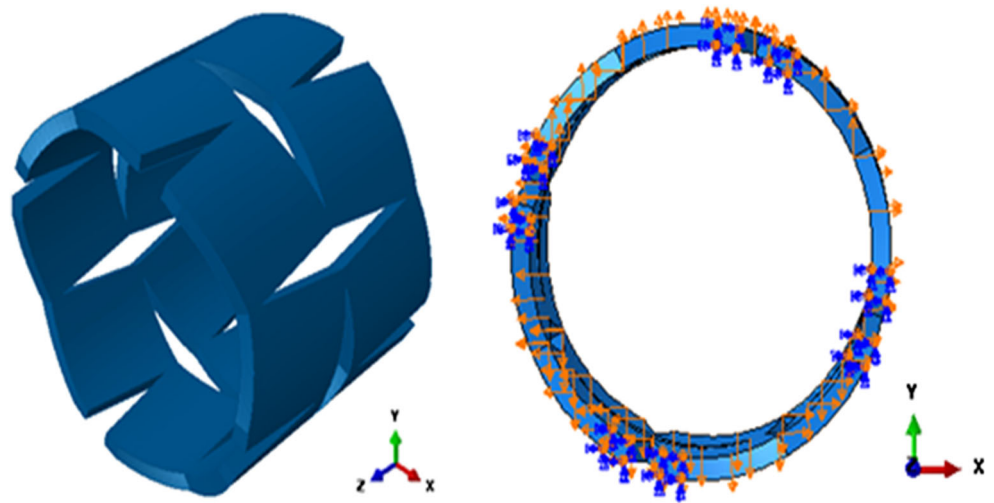
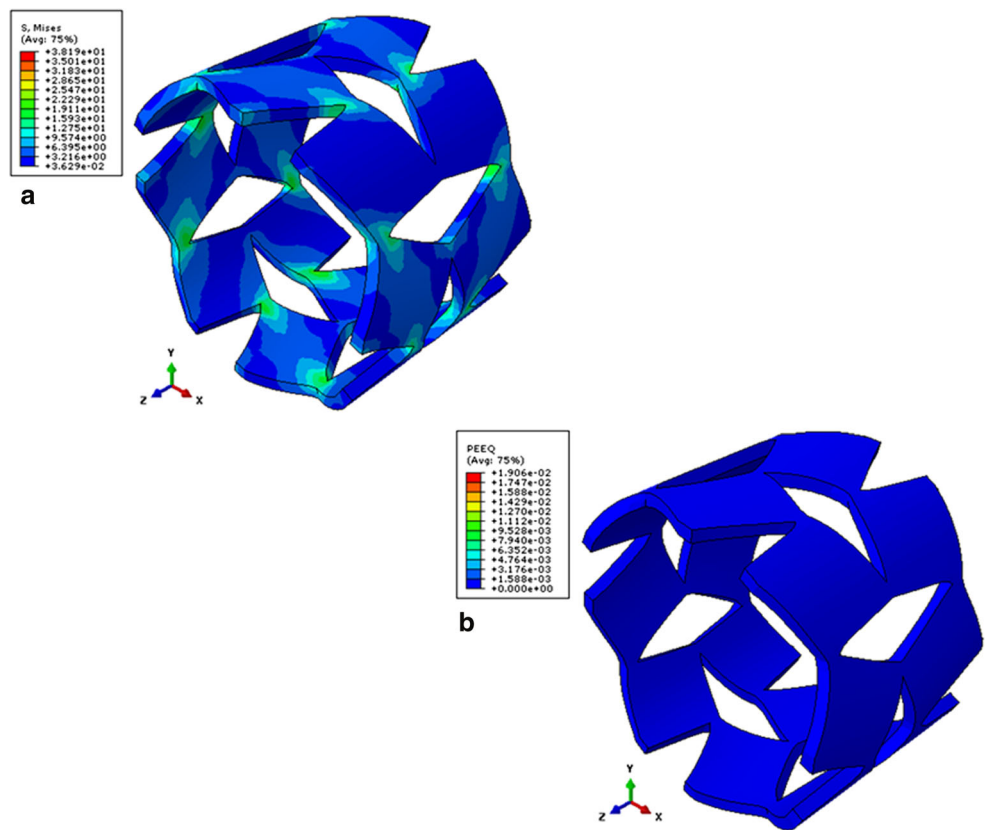


Fig. 55 a Von Mises stress of the plastically deformed Auxetic-ring model, **b** PEEQ of the FEA model when yielded



element model. The FEA model was built with the same structural and dimensional details as the physical Auxetic stent. To simplify the model symmetry was assumed along the length and therefore, only one unit-cell (comprising of four rotating-squares) was deliberately incorporated into the FEA model. The Auxetic-ring model was created to allow the diametrical changes to be carefully examined in this analysis, and also because to mesh the whole Auxetic stent would require significant computational resources and solution time owing to the complex geometry of the Auxetic stent (Fig. 53).

The same material (elastic–plastic) data was assigned to the FEA model, which was acquired earlier from the baseline tensile testing of the rigid polyurethane material of 75 shore D hardness. Radial displacements were applied in small increments outwardly from the inner luminal side of the model instead of radial pressure as shown in Fig. 54. A range of radial resultant reaction forces were collected at small increments of radial displacement applied outwardly from the lumen of the Auxetic-ring model. These reaction forces were subsequently used to calculate pressure values

at small increments of radial displacement (extension) of the model. The calculated radial pressure values with their respective radial displacement values of the FEA model were subsequently compared with the results of the physical stent-expansion Test-III.

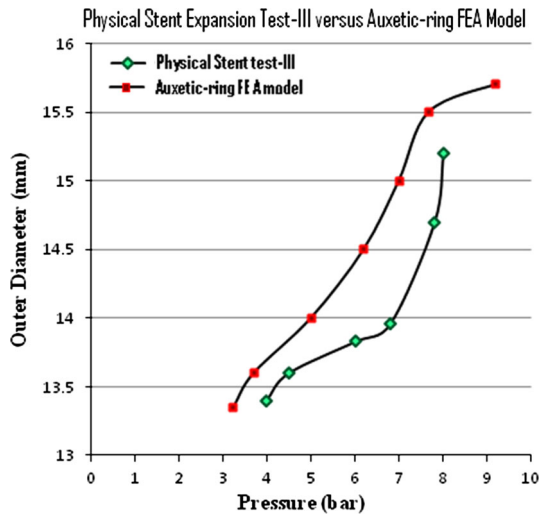


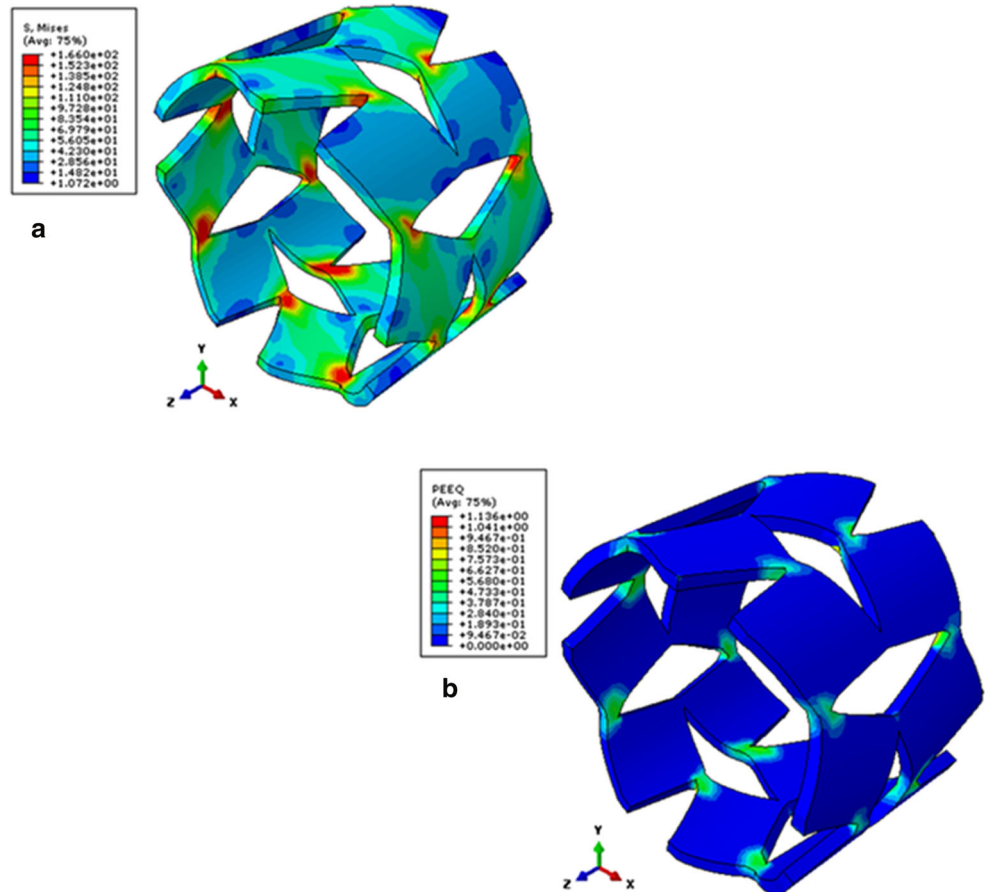
Fig. 56 Comparison of Physical Stent Expansion Test-III with the results of the Auxetic-ring FEA model

It was found from the Von Mises stress and equivalent plastic strain (PEEQ) values that the Auxetic-ring model started yielding or deforming plastically when 0.35 mm radial displacement was applied outwardly from the inner lumen of the model and the radial pressure at this point was calculated as 3.24 bar. As the maximum Von Mises stress observed in the model at this pressure was found to be 38.19 MPa, which was slightly higher than the yield strength of the polyurethane material (i.e. 37.5 MPa), and the equivalent plastic strain collected from the contour legend was 0.0196 (i.e. maximum plastic strain was about 1.90 %) as illustrated in Fig. 55. The finite element modelling results comprising of a range of radial pressure values calculated at different radial displacement values applied to the model, were subsequently compared with the results of the physical stent expansion Test-III as shown in the Fig. 56.

Since, it was established previously from the stent expansion Test-III that the Auxetic oesophageal stent failed at 8.3 bar pressure. Therefore, it was found that when radial displacement of 2.7 mm was applied to the model, the radial pressure was calculated as 9.2 bar (from the reaction force values).

Therefore, the maximum Von Mises stress of the FEA model (at 9.2 bar radial pressure) reported from the contour

Fig. 57 a Von Mises Stress contour plot of the model where the model is assumed to have ruptured and **b** an equivalent plastic strain of the model



legend (in Fig. 57), was 166 MPa which was equal to the maximum yield stress or the ultimate tensile strength of the model material. Consequently, the Auxetic-ring model was theoretically assumed as having failed at this point. The equivalent plastic strain (PEEQ) found from the contour legend was 1.136 (i.e. maximum plastic strain was around 113 %) as shown in Fig. 57.

It was established from the comparative data plotted in the graph in Fig. 56 that the agreement between the physical stent expansion behaviour and the simulated Auxetic-ring FEA model was satisfactory, even though the rigid polyurethane material used for the fabrication of the physical Auxetic stent and for the Auxetic-ring FEA model was different.

4 Conclusions

The outcome of the comparative analysis which was carried out based on the results obtained from the manufacturing and surface characterisation study, clearly showed that the lasercutting method is an effective and rapid way of producing Auxetic films. It was also established that instead of fabricating seamed Auxetic stent by using lasercut Auxetic film, lasercutting of polyurethane tubes for the production of seamless Auxetic stent, will not only avoid the problem of having weak welded joints but also the production time of the Auxetic stent can also be reduced. The production of seamless Auxetic oesophageal stent by vacuum casting technique was found to be effective and less time-consuming. The results from the mechanical characterisation of the Auxetic films and seamless Auxetic stents; identified the force values which were involved in their elastoplastic deformations, and determined their mechanical properties and plastic (permanent) deformation behaviour. Finite element models of both Auxetic film and oesophageal stent were developed, and compared with the experimental results with a good agreement.

It was established from the stent expansion tests using semi-rigid and rigid Auxetic stents that, semi-rigid Auxetic stent tend to expand (both radially and longitudinally) more than rigid Auxetic stent. This is due to several reasons including the (i) rigid Auxetic stent being too stiff and failing early (at low pressure increments), (ii) there being more squares with an increase in the number of corresponding plastic hinges as eight squares or hinges are present circumferentially in the semi-rigid Auxetic stent compared to just six in the rigid Auxetic stent and (iii) the diamond-shaped (hollow) spaces of the semi-rigid stent were narrower (at 1 mm width) when compared to the spaces in rigid stent which were 2 mm wide. Therefore, it was found from this study that the rotation or hinging

mechanism of the individual units and their size or angle, played a vital role in the overall expansion of the Auxetic (rotating-squares) network. Additionally, it is also envisaged that an Auxetic oesophageal stent exhibiting an anisotropic mechanical behaviour will conform well to the multi-layered oesophageal wall having a non-linear anisotropic mechanical response.

References

- McCabe ML, Dlamini Z. The molecular mechanisms of oesophageal cancer. *Int Immunopharmacol.* 2005;5(7–8):1113–30.
- Lerut T, Stamenkovic S, Coosemans W. Obstructive cancer of the oesophagus and gastroesophageal junction. *Eur J Cancer Suppl.* 2005;3(3):177–82.
- Lamb PJ, Griffin SM. The anatomy and physiology of the oesophagus. London: Springer; 2006.
- Natali AN, Carniel EL, Gregersen H. Biomechanical behaviour of oesophageal tissues: material and structural configuration, experimental data and constitutive analysis. *Med Eng Phys.* 2009;31:1056–62.
- Yang W, Fung TC, Chian KS, Chong CK. Three-dimensional finite element model of the two-layered oesophagus, including the effects of residual strains and buckling of mucosa. *Proc Inst Mech Eng Part H J Eng Med.* 2007;221(H4):417–26.
- Pope CE, Horton PF. Intraluminal force transducer measurements of human esophageal peristalsis. *Gut.* 1972;13(6):464–70.
- Schoen HJ, Morris DW, Cohen S. Esophageal peristaltic force in man—response to mechanical and pharmacological alterations. *Am J Dig Dis.* 1977;22(7):589–97.
- Pennathur A, Chang AC, McGrath KM, Steiner G, Alvelo-Rivera M, Awais O, Gooding WE, Christie NA, Gilbert S, Landreneau RJ, Luketich JD. Polyflex expandable stents in the treatment of esophageal disease: initial experience. *Ann Thorac Surg.* 2008;85(6):1968–73.
- Schoppmann SF, Langer FB, Prager G, Zacheri J. Outcome and complications of long-term self-expanding esophageal stenting. *Dis Esophagus.* 2013;26(2):154–158.
- Grima JN, Evans KE. Auxetic behavior from rotating squares. *J Mater Sci Lett.* 2000;19(17):1563–5.
- Attard D, Manicaro E, Gatt R, Grima JN. On the properties of Auxetic rotating stretching squares. *Physica Status Solidi B [Basic Solid State Physics].* 2009;246(9):2045–54.
- Grima JN, Farrugia PS, Caruana C, Gatt R, Attard D. Auxetic behaviour from stretching connected squares. *J Mater Sci.* 2008;43(17):5962–71.
- Ali MN, Rehman IU. An Auxetic structure configured as oesophageal stent with potential to be used for palliative treatment of oesophageal cancer; development and in vitro mechanical analysis. *J Mater Sci Mater Med.* 2011;22(11):2573–81.
- Mohan V, Kozarek RA. Placement of conventional and expandable stents for malignant esophageal stenosis. *Tech Gastrointest Endosc.* 2001;3(3):166–75.
- Sabzi M, Mirabedini SM, Zohuriaan-Mehr J, Atai M. Surface modification of TiO₂ nano-particles with silane coupling agent and investigation of its effect on the properties of polyurethane composite coating. *Prog Org Coat.* 2009;65:222–8.
- Grima JN, Manicaro E, Attard D. Auxetic behaviour from connected different-sized squares and rectangles. *Proc R Soc Math Phys Eng Sci.* 2011;467(2126):439–58.